Acta Geologica Polonica, Vol. 64 (2014), No. 2, pp. 189–206
DOI: 10.2478/agp-2014-0011

An early Middle Anisian (Middle Triassic) *Tubiphytes* and cement crusts-dominated reef from North Dobrogea (Romania): facies, depositional environment and diagenesis

LIVIA POPA[1, 3], CRISTINA E. PANAIOTU[2] AND EUGEN GRĂDINARU[1]

[1]*Department of Geology, Faculty of Geology and Geophysics, University of Bucharest, Bd. Bălcescu Nicolae 1, RO-010041 Bucharest, Romania.*
E-mails: livia.dobre@gmail.com; eugen.gradinaru@g.unibuc.ro
[2]*Department of Mineralogy, Faculty of Geology and Geophysics, University of Bucharest, Bd. Bălcescu Nicolae 1, RO-010041 Bucharest, Romania.*
E-mail: cris.panaiotu@gmail.com
[3]*OMV Petrom S.A., Reservoir Management Department, Asset IV Moesia South, 22nd Coralilor Street, 013329, Bucharest, Romania.*

ABSTRACT:

Popa, L., Panaiotu, C.E. and Grădinaru, E. 2014. An early Middle Anisian (Middle Triassic) *Tubiphytes* and cement crusts-dominated reef from North Dobrogea (Romania): facies, depositional environment and diagenesis. *Acta Geologica Polonica*, **64** (2), 189–206. Warszawa.

A well-developed Triassic carbonate platform is exposed in the eastern part of the Tulcea Unit, in the Cimmerian North Dobrogean Orogen, southeastern Romania. Facies analysis of the 200 m thick succession of lower Middle Anisian limestones exposed in a large limestone quarry south of the village of Mahmudia suggests a transition from upper slope towards toe-of-slope carbonate facies, reflecting sea-level fluctuations and tectonic tilting. The slope is dominated by *in situ* microbialites in the upper portion, consisting of reefal boundstone facies, and by molluscan coquina and cement boundstones. A key role is played by the cosmopolitan micro-encruster *Tubiphytes*, which became common in the aftermath of the mass extinction at the Permian/Triassic boundary, and by autochthonous micrite and synsedimentary marine cement. The absence of metazoan reef builders, such as sponges and corals, reflects the fact that microbes were the first organisms to recover after the Permian/Triassic crisis under unusual marine conditions and that their main role in reef formation was sediment stabilization along the upper slopes. The lower slope is mostly detrital, being dominated by platform-derived bioclastic rudstones and crinoidal floatstones, which are interbedded with basinal carbonate hemipelagics. The toe-of-slope is composed of pelagic wackestones framed by thin tongues of intraclast breccia. All these observations are in agreement with the slope-shedding model described for the Pennsylvanian microbial margin in Asturias (northern Spain) and the Anisian–Ladinian flat-topped, steep-rimmed Latemar platform (Dolomites, Italy).

As most of the Anisian reefs were described from western and eastern Tethys (Southern Alps, Hungary, China), the occurrence of the early Middle Anisian *Tubiphytes*-reef from North Dobrogea (Romania) contributes to resolving the puzzle of the geographic distribution of reef recovery in the Middle Triassic.

Key words: Anisian (Middle Triassic); Carbonate slope; Microbialites; *Tubiphytes*-buildup; North Dobrogea; Romania.

INTRODUCTION

The dominance of microbial carbonates seems to be the main characteristics of carbonate buildups during times of skeletal metazoan crisis after extinction events (Webb 1996). This is recorded after the end-Palaeozoic or Early–Middle Triassic extinctions (Della Porta *et al.* 2004), which deeply affected the carbonate production in the following time intervals. The Early Triassic 'reef gap' lasted more than 5 Ma (Payne *et al.* 2006), before the reef communities re-diversified during the Middle Triassic (Flügel and Stanley 1984; Stanley 1988; Senowbari-Daryan *et al.* 1993; Flügel 1994, 2002). During this time, the intense hothouse climate that caused the extinction persisted and the equator to pole temperature gradient was very low (Preto *et al.* 2010). The dry climate that generally dominated the earliest Triassic was interrupted later by a few moister phases, such as the one during the Middle Anisian (Stefani *et al.* 2010; Preto *et al.* 2010), revealing the unstable and pulsatory character of the environmental conditions.

A key role in the biotic evolution of the Triassic was played by the warming trend noted throughout this period, causing a reduction in the proportional contribution of microbes versus scleractinian corals in reef construction and an increase in the latitudinal extent of the tropical reefs (Kiessling 2010).

The present paper deals with *in situ* upper slope boundstones belonging to an M-carbonate factory (one of the three carbonate factories identified by Schlager 2000, 2003), dominated by microbial precipitation. This facies is equivalent to non-skeletal microbialite, one of the four categories into which reef frameworks were divided by Webb (1996). According to this author, the microbial buildup represents a non-enzymatic framework.

The studied constructional reef from Mahmudia, North Dobrogea, composed of microbial boundstones, is referred to herein as a biostrome (according to Kiessling *et al.* 1999 classification), as no apparent depositional high relief can be inferred in the field. It was formed by a micro-framework consisting of *Tubiphytes*, very small encrusting and low-growing organisms, as well as abundant fine-grained internal sediment, microbial crusts, and autochthonous micrite (automicrite), all reinforced by large volumes of marine cement, showing similarities with both Permian (Wood 1999, 2000; Weidlich 2002) and Ladinian reefs (Flügel 2002). From a compositional point of view, the *Tubiphytes*-reef is a microbial reef, one of the eight major compositional reef types distinguished by Flügel (1994, 2002).

Starting with the early Middle Anisian bioconstruction in Mahmudia, the reefs expanded throughout the Northern Tethys, the area being considered as reef-free during that time (e.g. Flügel 2002). From this perspective, the *Tubiphytes*-buildup from North Dobrogea is one of the few early Middle Anisian reefs known from the Tethys, thus completing the geological and geographical extension of this type of construction throughout this major marine domain.

The present paper gives the sedimentological characteristics of the Middle Triassic carbonate platform located in the easternmost part of the Tulcea Unit, North Dobrogea (Romania), with the aim of assessing the stratigraphic architecture, facies pattern and depositional environments of the Anisian sequence in the context of biotic recovery after the Permian/Triassic extinction. The role of diagenesis is highlighted as well.

GEOLOGIC AND STRATIGRAPHIC SETTING

The Triassic carbonate platform of the Tulcea Unit is located in the eastern part of the North Dobrogean Orogen (Text-fig.1). This orogen represents the westernmost segment of the Palaeo-Tethyan Cimmeride orogenic system (Text-fig. 1, inset), which continuous to the east into the Mountainous Crimea and the Greater Caucasus (Şengör 1984, 1986).

The North Dobrogean Orogen is built up of several tectonic units, making up a pile of northeasterly-verging high-angle overthrusts, or nappes. From south to north the following units were distinguished: Măcin (the uppermost), Consul, Niculiţel, and Tulcea (the lowermost) (Text-fig. 1). Whereas both innermost units (Măcin and Consul), and the outermost (Tulcea) unit are continental, basement-sheared nappes including relicts of a Variscan Orogen, the median unit (Niculiţel) is interpreted as a suture zone, based on the extensive occurrence of Middle Triassic basaltic rocks (Săndulescu 1995; Visarion *et al.* 1990).

The Triassic succession of the North Dobrogean Orogen is of Tethyan type, in contrast to the Germanic-type Triassic of the Moesian and Scythian platforms (Grădinaru 1995, 2000), lying to the south and north of the North Dobrogean Orogen (Text-fig. 1) respectively. The puzzling position of the North Dobrogean Triassic in the foreland of the Alpine Carpathian Orogen can be interpreted as a result of post-Triassic large-scale horizontal displacements of Tethyan terranes in close connection with the opening of the West Black Sea Basin (e.g. Grădinaru 1988; Okay *et al.* 1994; Banks and Robinson, 1997).

The studied Middle Anisian Mahmudia section is exposed in a 1.5-km long quarry for limestone used in

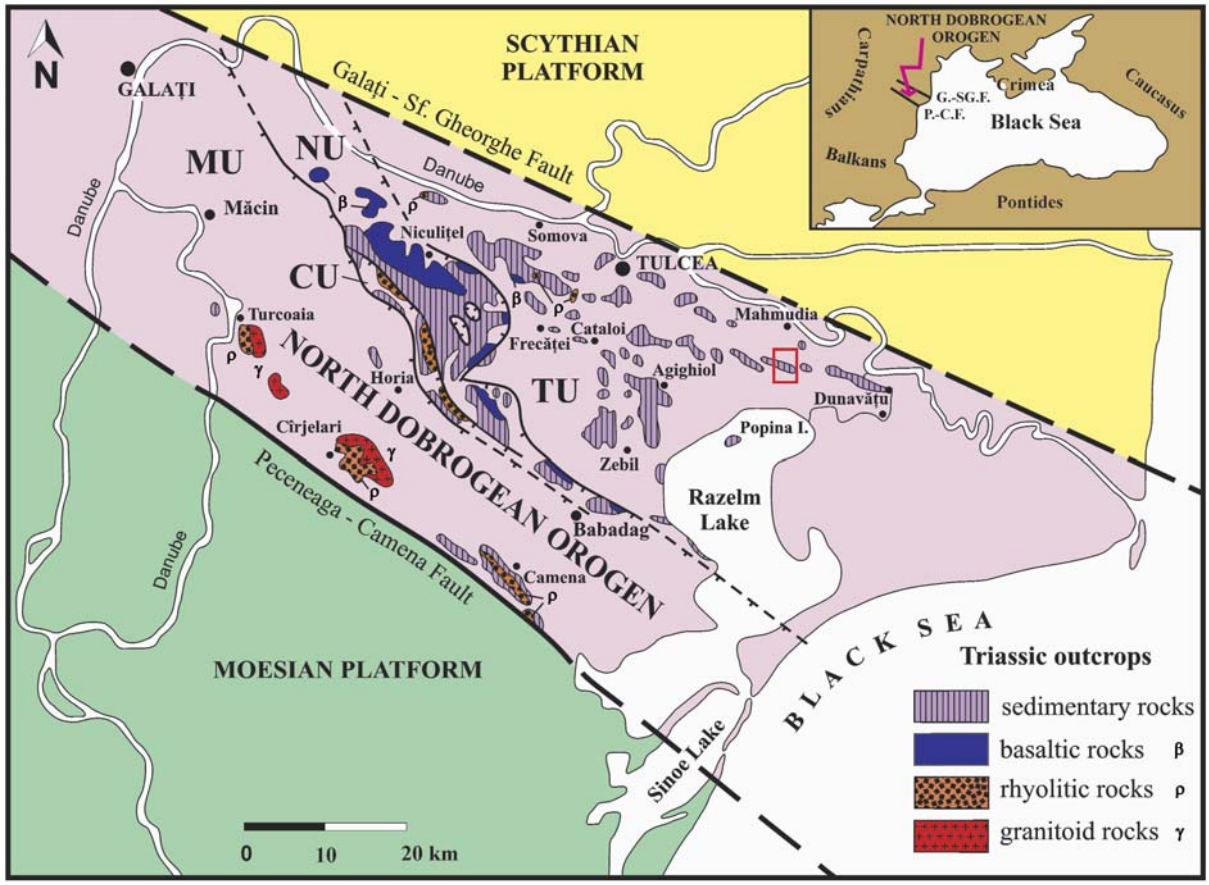

Text-fig. 1. Tectonic sketch map of the North Dobrogean Orogen, showing the occurrences of the Triassic rocks: **MU** – Măcin Unit, **CU** – Consul Unit, **NU** – Niculițel Unit, **TU** – Tulcea Unit (modified after Grădinaru 2000). The study area is shown by a red box. Inset map shows the geological setting of the North Dobrogean Orogen

the iron and steel industry. The quarry is located in the Caeracul Mare Hill area (N45°03'12.41'', E29°03'34.52'') south of the village of Mahmudia, 35 km east of Tulcea (Text-fig. 2). The exposed carbonate rocks represent the Caerace Formation. Due to block faulting and the quarrying activity, the stratigraphic succession in the quarry is highly disturbed. Similarly, due to poor exposure, the details of the geometry of the *Tubiphytes*-buildup remain unclear. The samples were taken from a 200-m thick succession exposed in a vertical wall in the northeastern corner of the quarry (Text-fig. 3).

The early Middle Anisian (Bithynian, in the European Triassic time scale; e.g. Shevyrev 1990; Mietto and Manfrin 1995) age of the *Tubiphytes*-buildup in the Mahmudia Quarry is documented by the ammonoid fauna (Grădinaru, in prep.), including *Robinsonites* sp., *Unionvillites* sp., *Alanites* sp. aff. *A. visendus* Shevyrev, *Gymnites* sp. aff. *G. tozeri* Bucher, *Megaphyllites prometheus* Shevyrev, *Longobarditoides solimani* (Toula), *Hollandites silberlingi* Bucher, *Caucasites inflatus* Shevyrev, *Acrochordiceras hyatti* Meek, *Ussurites* sp. aff. *U. arthaberi* (Welter), etc. This fauna indicates the lower Middle Anisian Osmani Zone of the North-Western Caucasus (Shevyrev 1995) and the lower Middle Anisian Hyatti Zone of Western Nevada (Silberling and Nichols 1982; Bucher 1992; Monnet and Bucher 2006). The macrofauna associated with the *Tubiphytes*-buildup also includes rich coiled nautiloids, abundant and diverse bivalves and gastropods, and less diverse brachiopods.

MATERIALS AND METHODS

From the measured section, more than 150 samples were collected (see sample location in Text-fig. 4) and 70 thin sections and polished slabs were prepared for petrographic analysis by polarized light microscopy, UV fluorescence microscopy and cold cathodoluminescence microscopy (CITL). Small polished slabs, mainly from the cement-rich parts, were etched with diluted acetic acid and studied with a scanning electron microscope (SEM). Other larger polished slabs were

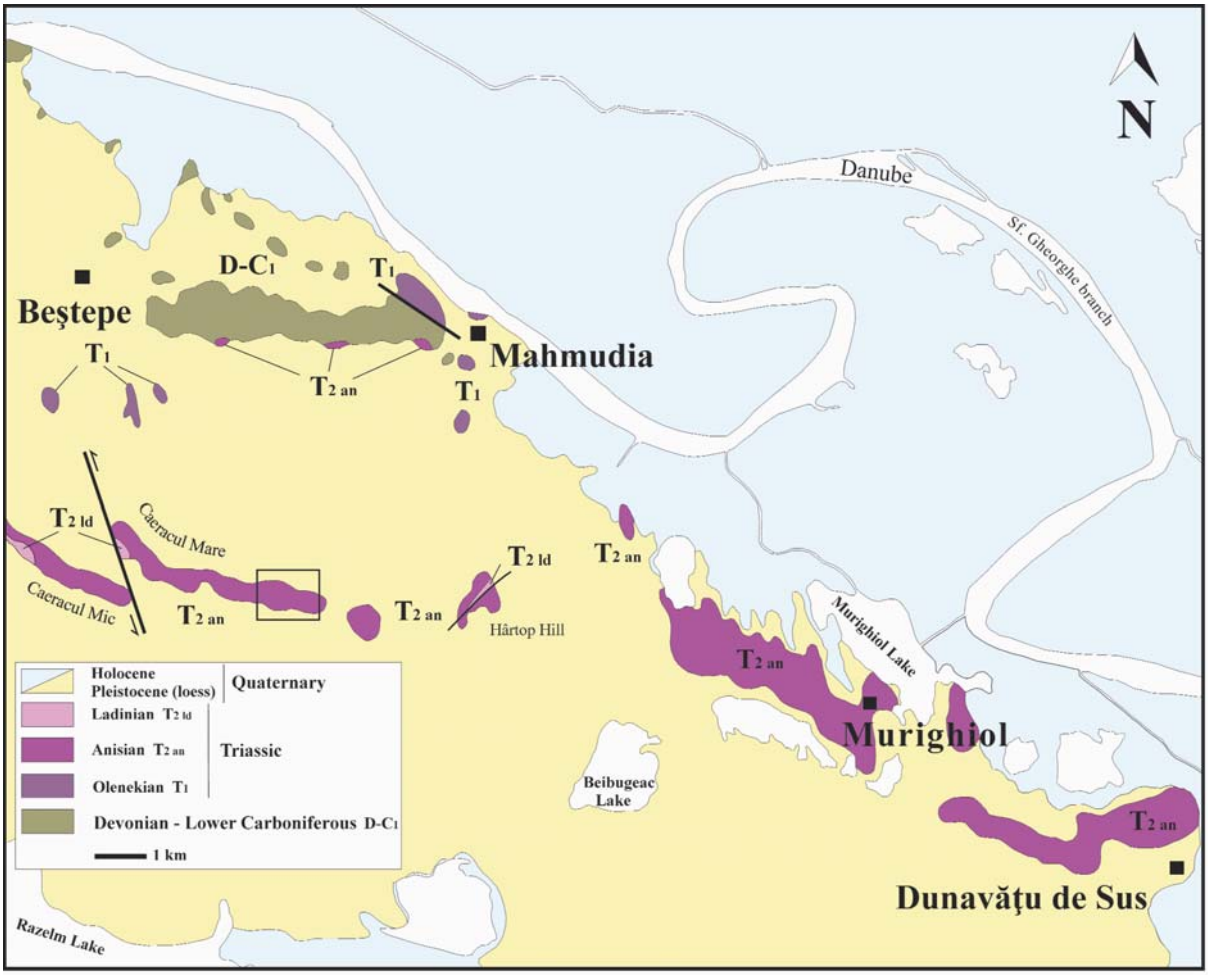

Text-fig. 2. Geologic map of the Mahmudia region (modified after Mirăuţă and Panin 1976). The study area is shown by a black box

etched with 10% HCl, stained with alizarine and potassium ferricyanide, and fingerprinted on acetophane peels in order to detect the mineralogy of the different carbonate components. Carbon and oxygen stable isotopes were measured on samples taken from polished slabs with a handheld micro-drill. The powders were reacted with 100% phosphoric acid at 75˚C, and the evolved CO_2 gas was analyzed with a Finnigan MAT 251 mass spectrometer. The $\delta^{13}C$ and $\delta^{18}O$ values are corrected according to the NBS19 standard and re-

Text-fig. 3. The carbonate deposits of the Middle Triassic Caerace Formation exposed in northeastern corner of the Caeracul Mare Hill sector of the Mahmudia Quarry, with the stratigraphic section detailed in the lithofacies column (B) in Text-fig. 4. The main lithofacies detailed in Table 1 are overwritten (**S1** – *Tubiphytes* boundstone; **S2** – bivalve coquina with automicrite; **S3** – cemented-dominated boundstone; **S4** – bioclastic rudstone; **S5** – laminated bindstone; **S6** – crinoidal floatstone; **S7** – intraclast breccias; **S8** – pelagic wackestone)

ported in per mill (‰) relative to the V-PDB (Vienna-PeeDee Belemnite) standard (standard deviation smaller than 0.04‰).

CARBONATE FACIES BELTS AND THE *TUBIPHYTES*-BUILDUP FRAMEWORK

The Caerace Formation is subdivided into a number of lithological units (in ascending stratigraphic order): massive dolostone, pelagic dolomitized limestone, stromatactis limestone, bioclastic limestone, nodular limestone, reefal (*Tubiphytes*) limestone and pelagic limestone, some of them recurring in the succession (Text-fig. 4). A depositional slope with three facies belts (upper slope, lower slope and toe-of-slope, and its transition to basinal sediments) can be distinguished in the studied sequence that includes the *Tubiphytes*-buildup.

Macroscopically, the reefal (*Tubiphytes*) limestone is strongly compacted with poorly developed sedimentary structures. The depositional slope sequence, as shown in Table 1, consists of: (1) Upper slope, 120 m of massive limestones incorporating *Tubiphytes* boundstones, molluscan coquina and cement boundstones, without any evidences of subaerial exposure; 2) Lower slope, 40 m thick, dominated by bioclastic rudstones and crinoidal floatstones, which are interbedded with carbonate hemipelagics; 3) Toe of slope, 30 m thick, mainly composed of thin intraclastic breccia tongues framing pelagic wackestones and peloidal bindstones.

Facies types

***Tubiphytes* boundstone [S1]** (Pl. 1; Pl. 2; Pl. 3, Figs 1, 2) is the dominant facies, representing *in-situ* accumulation with the highest growth potential. It has a massive appearance and mound morphology (Pl. 1, Fig. 1). Its fossiliferous zones are rich in bivalves (lithofacies S2), ammonoids, nautiloids, numerous gastropods and rare brachiopods. In parts *Tubiphytes* is embedded in marine cement 2–3 cm thick (Pl. 1, Figs 2, 4).

The main biotic constituent of this facies consists of ramose individuals of the problematic organism *Tubiphytes* (up to 2 cm long, Pl. 2; Pl. 3, Fig. 2), a common fossil of the Anisian reef assemblages. Also important are local concentrations of ostracods, foraminifera, thin-shelled bivalves, brachiopods (Pl. 2, Fig. 2) and crinoids, all embedded in large amounts of isopachous fibrous cm-thick cements (Pl. 1, Fig. 5; Pl. 2, Fig. 1; Pl. 3, Fig. 2).

The framestone is characterised by the abundance of *Tubiphytes* in growth position (see Enos *et al.* 2006), the prominence of encrusting organisms (*Tubiphytes* and foraminifera, Pl. 1, Fig. 5; Pl. 2, Fig. 1), the massive macroscopic appearance and the abundance of constructional pores (growth-framework porosity of Croquette and Pray 1970), which reach up to 50% of the rock volume.

Biogenic crusts with clotted peloidal fabric and gravity-defying structures evolved around *Tubiphytes* (Pl. 2, Fig. 1). Internal sediment is present in considerable amounts, exposing peloidal textures with traces of possibly microbial filaments (Pl. 1, Fig. 5, inset detail) which, together with the automicrite (Pl. 2, Figs 3–5; Pl. 3, Fig. 1), could have been biologically mediated. Bioturbation is also present (Pl. 3, Fig. 1).

Cements make up to 50% of the total rock volume. The cement sequence is: fibrous calcite, radiaxial fibrous calcite (RFC) and drusy cement (now all low-magnesium calcite - LMC). Isopachous crusts of brown bladed or fibrous crystals are by far the most common cement within the boundstone facies with growth framework porosity. Thin micrite films ('dust lines') are intercalated by different cement generations (Pl. 2, Fig. 1).

Mm- to cm-thick crusts consisting of RFC, growing on an extended *Tubiphytes* framework, are common within the boundstones (Pl. 1, Figs 2, 3). In some cases dissolution preceded its precipitation, as demonstrated by the truncation of the sedimentary fabric in the surrounding boundstone facies (Pl. 2, Fig. 1). Isopachous RFC cement often contains dark and light coloured zones indicating several episodes of cement precipitation. Fluorescence investigations show alternations of fluorescent and non-fluorescent laminae (Pl. 8, Fig. 6). Equant sparry calcite is a minor component of the boundstone facies found within framework voids that remained after marine syndepositional cementation (Pl. 2, Fig. 3; Pl. 3, Figs 1, 2; Pl. 8, Fig. 8).

Bivalve coquina with automicrite [S2] (Pl. 3, Figs 3–6) is interbedded with *Tubiphytes* boundstone, and consists of thin-shelled bivalves, rarely brachiopods, gastropods, ammonoids, and ostracods. The bivalves are microbially encrusted (Pl. 3, Fig. 5). Some of the bivalve shells are preserved with both valves, including internal shell structures. Their internal cavities were filled partially with peloidal cement, before embedment in fibrous cement (Pl. 3, Fig. 6). The automicrite, the other component of the microfacies, is characterized by clotted peloid aggregates without traces of bedding (Pl. 3, Figs 3, 4).

Cement boundstone [S3] (Pl. 3, Figs 7, 8; Pl. 7, Figs 1–4) consists of cm-scale cement arrangements with rare

patches of automicrite and thin-shelled bivalves. Recrystallized fibrous cement prevails, followed by a band of scalenohedral dolomite cement ("dog-tooth cement" – DTC) (Pl. 8, Figs 1, 2). The remaining voids are filled by equant blocky calcite (Pl. 7, Fig. 1). The wavy micrite layers, intercalated by fibrous cement, mimic a distinct growth structure probably determined by organic mats (Keim and Schlager 1999). Black and white peloids (Pl. 3, Figs 7, 8), viewed in stained thin section, have a low magnesium calcite (LMC) centre and a dolomite rim. Automicrite occurs in small patches (Pl. 7, Figs 1, 2, 4). Stromatactis structures are spotted in some samples (Pl. 7, Fig. 4) marking cavities with a flat floor, composed of peloids, and a digitate top, filled by RFC and blocky calcite. These reveal the sedimentation sequence.

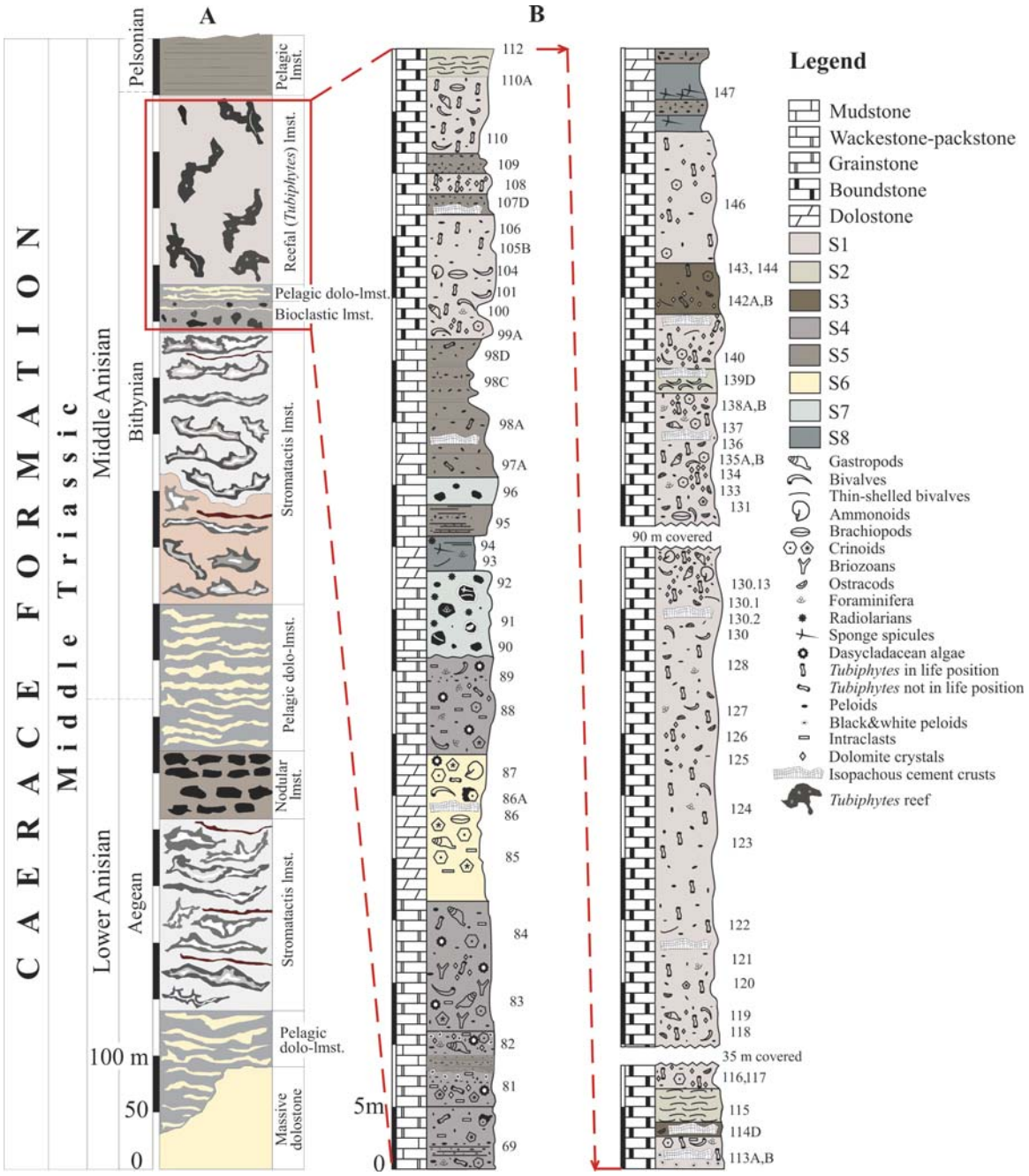

Text-fig. 4. Synthetic lithological column (**A**) of the Middle Anisian Caerace Formation in the Mahmudia Quarry, and detailed lithofacies column (**B** continued) of the studied section (marked by the red quadrangle) with sample log for the lower Middle Anisian (Bithynian) *Tubiphytes*-buildup. Symbols S1 to S8 as shown in Text-fig. 3 and Table 1

Bioclastic rudstone facies [S4] (Pl. 4; Pl. 5, Figs 1–6) is generally structureless, sometimes with clotted peloidal micrite inside cryptic cavities, and is occasionally interbedded with laminated mudstones that represent basinal carbonate hemipelagics. A wide range of bioclasts is common: crinoids, bivalves, gastropods,

Facies belt	Name	Lithofacies type	Texture, Composition	Microbial fabric	Depositional environment
Slope	S1	***Tubiphytes* boundstone**	*Tubiphytes* ramose framework, foraminifera, ostracods, gastropods, bivalves, brachiopods, ammonoids, nautiloids, internal sediment, micritic crusts, isopachous cement, selective dolomitization.	Internal sediment and automicrite. Foraminiferal encrustations. *Tubiphytes.*	Upper slope
	S2	**Bivalve coquina with automicrite Cement dominated boundstone**	Coquina composed of bivalve shell beds.	Automicrite and shell encrustations.	Upper slope
	S3		Isopachous radiaxial fibrous cement crusts, micritic thin films, rare *Tubiphytes* and stromatactis. Dolomitization.	Microproblematic unknown structures. Automicrite. Black and white peloids (*Muranella*)	Upper slope
	S4	**Bioclastic rudstone**	Rudstone, crinoid fragments, bivalves, gastropods, *Tubiphytes*, bryozoans, foraminifera, juvenile ammonoids, brachiopods, dasycladacean algae, intraclasts. Thick radiaxial fibrous cement crusts and selective dolomitization affecting especially intraclasts.	Laminated fine-grained, stromatolite consisting of alternating peloid and micrite layers common in cryptic cavities	Lower slope
	S5	**Laminated bindstone**	Peloids alternating with micrite layers. No fossils observed.	Irregular micrite laminae as interbeds	Geopetal infilling
	S6	**Crionoidal floatstone**	Whole fossils: brachiopods, gastropods, juvenile ammonoids and large crinoidal parts (columnals, stems), dolomitized micrite matrix.	Irregular microbial encrustations and oncoids	Slope, reef flanks, precursor reef stage
	S7	**Intraclast breccia**	Nodules and matrix are pelagic microbioclatic wackestones.		Toe of slope
Basin	S8	**Pelagic wackestone**	Wackestone with thin-shelled bivalves, sponge spicules, ostracods, radiolarians, pelagic foraminifera and rare crinoidal fragments, burrows - alternating with dolomite layers (2-3 cm).		Basinal sediments

Table 1. Facies and facies associations, and related depositional environments, of the lower Middle Anisian section of the Caerace Formation in the Mahmudia Quarry, North Dobrogea

dasycladacean algae, bryozoans, foraminifera and *Tubiphytes*. Intraclasts, showing soft edges and plastic deformations, are also present and are often dolomitized (Pl. 4, Figs 1–5; Pl. 5, Figs 1–4; Pl. 7, Fig. 5, 6).

The foraminiferal assemblage includes Duostominidae, biserial foraminifera (Earlandinidae), multiserial types (Trochaminidae and Endotrianidae), encrusting *Geinitzina tcherdynzevi* Miklukho-Maklay (Pl. 4, Fig. 6; Pl. 5, Fig. 4) and *Meandrospira dinarica* Kochansky-Devidé and Pantić, a typical foraminifer in the Anisian carbonate platforms of the Tethyan realm (Berra *et al.* 2005). Sessile foraminifera that encrust crinoid columnals (Pl. 4, Fig. 5), *Tubiphytes* specimens encrusted by foraminifera (Pl. 4, Fig. 5; Pl. 5, Fig. 3), gastropods (Pl. 5, Fig. 4) and juvenile ammonoids are observed as well. This facies contains the bryozoan *Reptonoditrypa cautica* Schäfer and Fois, in some cases enveloped by a micritic crust (Pl. 5, Fig. 2). Recrystallized and reworked dasycladacean algae are also present (Pl. 4, Fig. 6; Pl. 5, Fig. 1). An interesting feature of this facies is the occurrence of laminated geopetal infillings formed by alternations of irregular peloid and micrite laminae (Pl. 4, Fig. 6, right). Most of the peloids are bordered by calcite rims.

Large isopachous cement crusts, several cm-thick, which contain large intraclasts, interfinger with pelagic wackestones containing calcified radiolarians scattered in a muddy matrix (Pl. 5, Fig. 5).

Laminated bindstone (geopetal infilling) [S5] (Pl. 5, Fig. 2; Pl. 6, Fig. 6) consists of fine-grained laminated peloidal grainstone grading into peloidal packstone. The facies exhibits distinct alternations of thicker and thinner peloidal layers separated by irregular, probably microbial, micrite laminae (m).

Crinoidal floatstone [S6] (Pl. 5, Fig 7; Pl. 6, Figs 1–3) is intercalated within bioclastic rudstone and consists of a 10-m thick sequence with abundant crinoid stem fragments and arm plates, as well as subordinate brachiopods, gastropods and bivalves, embedded in an intensively dolomitized muddy matrix. Juvenile ammonoids are also present (Pl. 6, Fig. 1). Irregular micrite rims around crinoid columnals and stem plates or bivalve fragments (Pl. 5, Fig. 7; Pl. 6, Fig. 2) are common. The matrix consists of LMC microspar and small idiomorphic dolomite crystals, isolated or in aggregates (Pl. 5, Fig. 7, inset stained detail). Large fibrous cement crusts and stylolites (Pl. 6, Figs 1, 3) are characteristic of this facies.

Intraclast breccia [S7] (Pl. 6, Fig. 5) show a tectonic (faulted) contact with the adjacent bioclastic rudstone (Pl. 6, Fig. 4). Locally, m-thick intervals of finer grained (pelagic) carbonates, the S4 burrowed pelagic wackestone facies and S5 peloidal grainstones with uneven bedding-parallel laminae, are intercalated between breccia tongues. The breccias are composed of mud-supported calcareous clasts with diameters ranging between 1 mm and 10 cm, embedded in a dark-coloured pelagic microbioclastic wackestone. The clasts contain calcified radiolarians, sessile foraminifera, sponge spicules and thin-shelled bivalves, some of them being bordered by a thin cement rim (Pl. 6, Fig. 5).

Burrowed pelagic wackestone [S8] (Pl. 6, Figs 4, 6) with abundant fine pelagic and benthic biodetritus is c. 10 m thick. The microfossils, commonly sponge spicules, shell debris (thin-shelled bivalves), ostracods, uniserial foraminifera and calcified radiolarians, are sparsely distributed within a densely mottled matrix due to intensive burrowing (Pl. 6, Fig. 6). Locally, dense concentrations of sponge spicules occur, although no fossilized sponge body was ever found. Dolomitization affected especially the bioturbated and more porous layers, and did not affect the impermeable mud between the burrows.

Depositional environment

The eight facies recognised within the carbonate sequence of the studied section define a complex depositional environment. Based on facies associations and sedimentological processes that controlled carbonate production, the carbonate sequence can be divided into the following sub-environments.

Upper slope - microbial buildup. This part is almost exclusively represented by S1 and sporadically by S2 and S3 lithofacies. The homogeneous distribution of microbial limestones indicates their *in situ* origin, without sedimentological contribution from other parts of the platform.

The key component of the microbial buildup in the Middle Anisian Mahmudia section is the *Tubiphytes* micro-encruster, described previously as *Shamovella* (Riding and Guo 1992), a microproblematic with still debated affinities. While in the past it was considered an alga, a sponge or a bryozoan, recent studies showed this microorganism to be a cyanobacterial-foraminiferal association. The central cores of *Tubiphytes* consist of foraminiferal tubes (Pl. 2, Fig. 1, inset detail), belonging to Fischerinidae and Nubeculariidae or Nodobacullariinae (sessile species). The encrustations are variably dense tangles of clotted micrite considered to be microbially-mediated (Pratt 1995) and the laminated walls resulted from successive microbial mat encrustations (Pl. 2, Figs 1, 4, 5). It is unclear if the foraminifera were encrusted

in micrite while still alive or after death (Senowbari-Daryan *et al.* 2008). However, it is now considered as a *Tubiphytes*-like organism, attributed to the family Nigriporellidae Rigby, 1958 (Senowbari-Daryan 2013).

The *Tubiphytes* micro-encruster ("opportunistic communities" of Rollins and Donahue 1975, able to adapt to unstable environmental conditions; see Flügel 2002), did not contribute to reefs before the Permian, because the erect sessile foraminifera had not yet evolved (Pratt 1995; Senowbari-Daryan 2013), nor after the Jurassic, probably because of substrate competition. Environmentally, these reefs are regarded either as shallow (Senowbari-Daryan 2013) or deep-water (Pratt 1995). The lack of dasycladacean algae and other similar facies indicators suggest that the *Tubiphytes*-buildup described herein is rather deep-water.

Although *Tubiphytes* is claimed to be a secondary reef-builder (e.g. Emmerich *et al.* 2005), the prominent *Tubiphytes* occurrence is the most important feature in the lower Middle Anisian buildup in the Mahmudia Quarry. It is stated that the *Tubiphytes* micro-encruster enabled the stabilisation of carbonate sediments in the upper slope and allowed cement-rich reefs to flourish in the early Middle Anisian (Senowbary-Daryan *et al.* 1993; Enos *et al*. 2006). *Tubiphytes*-microbial buildups characterized mostly high relief depositional systems during the crisis periods of large skeletal-metazoans buildups. Examples are recorded from the Upper Devonian (Playford *et al.* 1989; Shen and Bao 1997), Lower Carboniferous (Mundy 1994), Upper Carboniferous (Della Porta *et al.* 2003), Permian (Bebout and Kerans 1993; Saller *et al.* 1999) and Middle Triassic

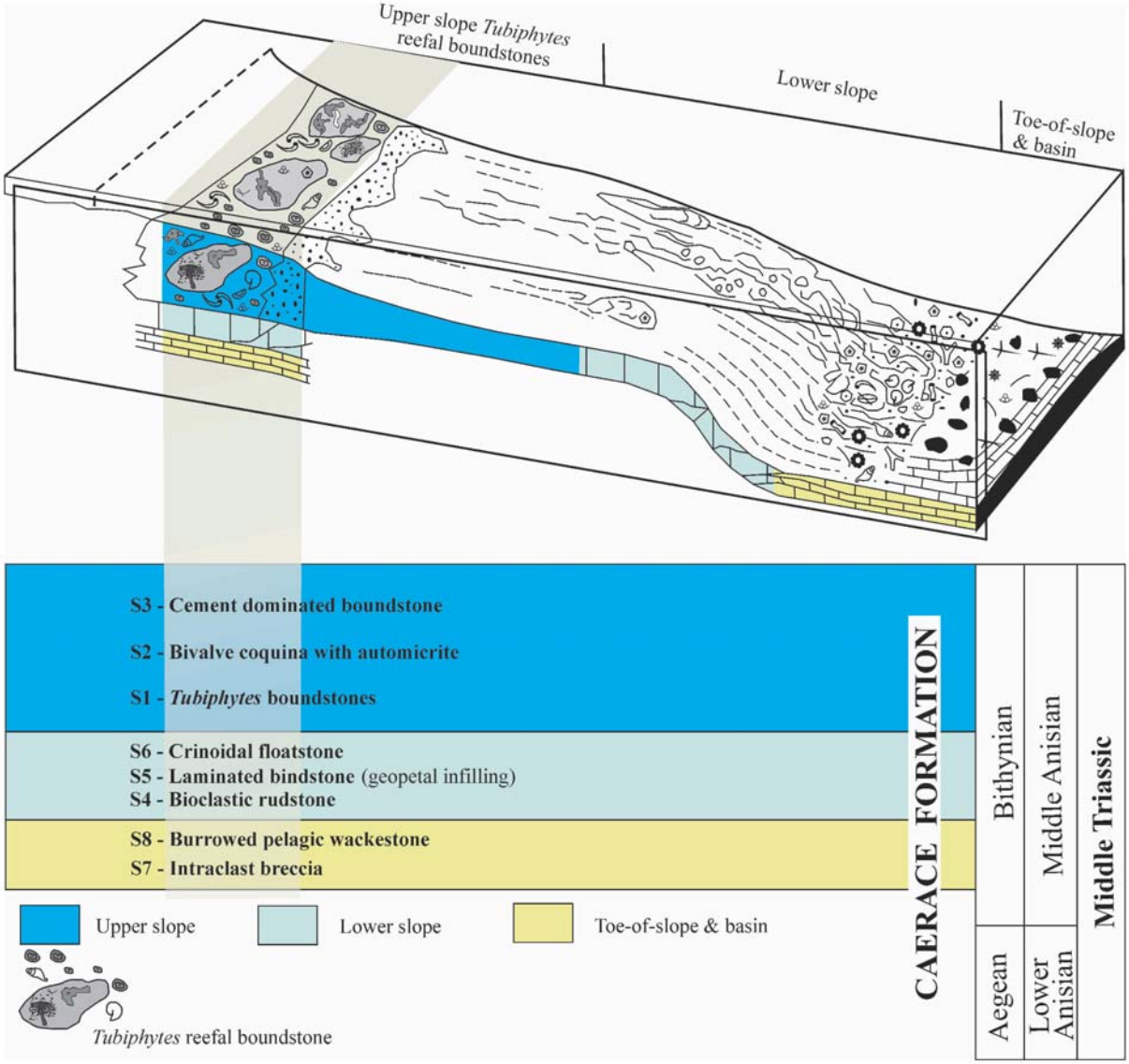

Text-fig. 5. Depositional model for the lower Middle Anisian (Bithynian) section of the Caerace Formation. Light grey shading marks the study section

(Keim and Schlager 2001; Marangon *et al.* 2011).

The automicrite, the other major component of the buildup, is very common in many ancient reefs, particularly in those older than the Cretaceous (Wood 2001). Generally, automicrite formation ranged from the outer part of the platform downslope to over 200 m depth (Keim and Schlager 1999; Della Porta *et al.* 2004).

A higher cementation rate characterizes reefs with higher rates of water agitation and a lower sedimentation rate (Lighty 1985). This is well confirmed by the studied low-growing *Tubiphytes* micro-encrusters. Thin micritic films, 'dust lines', intercalated through different cement generations (Pl. 2, Fig. 1), suggest that cementation occurred while the voids were still open to shallow marine waters (Payne *et al.* 2006).

Mollusc shell beds caught in large masses of fibrous cement (S2 lithofacies) are usually found in reefs and slopes due to current concentrations, storm wave and tempestite concentrations, or they represent transgressive lags or condensed horizons (Flügel 2010). A high abundance and taxonomic diversity of molluscs, especially bivalves, coiled nautiloids and other invertebrates, such as in the studied section, suggest high nutrient availability within the microbial reef. The mollusc shells and the cementation contributed together to the high-relief and rigid framework of the *Tubiphytes*-microbial buildup.

Large cement crusts (S3), up to 5 cm thick, are often found through the reef (Pl. 1, Figs 2, 3). They are associated with stromatactis structures (Pl. 7, Fig. 4), muddy sediment characterised by plastic texture, alternation of dark and light coloured lamina and dewatering structures (Pl. 7, Fig. 3). These structures, together with the lack of fossils, indicate an environment hostile to life, at few tens or even hundred metres depth.

Lower slope. It consists of lithofacies S4, S5 and S6. Microbial limestone is spotted through bioclastic rudstone, as rare *Tubiphytes* (Pl. 4, Figs 1, 2, 5; Pl. 5, Fig. 3), through laminated bindstone, as 'black and white peloids' (Pl. 3, Figs 7, 8; Pl. 4, Fig. 6), common in cryptic cavities of the Triassic reefs (Flügel 2010), and through crinoidal floatstone as micritic encrustations (Pl. 5, Fig. 7; Pl. 6, Fig. 2). The abundance of biotic encrustations, *Tubiphytes*, bryozoans, crinoids, and of amalgamated stromatolites, reveal a framework bioconstruction, resembling an initial reef, drowned either by rising sea-level or suffocated by overlying basinal sediments. Basinal influence may be inferred from interbedded laminated mudstones (Pl. 4, Fig 1), containing darker laminae with organic matter concentrations. Original topography is indicated by plasticity of the muddy sediment. The instability of the environment is suggested by large intraclasts incorporated into large cement crusts (Pl. 5, Fig. 5; Pl. 6, Fig. 3). Recrystallized and reworked dasycladacean algae, spotted in rudstone facies, were originally formed in the shallower-water platform top, an environment not identified in the study area. The crinoidal floatstone facies contributes to the stabilization of slopes and is common during the aggradational phase (Della Porta *et al.* 2004).

Toe of slope and basinal facies. The massive upper slope passes gradually into pelagic wackestone and intraclast breccia (lithofacies S7 and S8), with interspersed laminated bindstones. Compared with the other two facies, this one is very thin (c. 20 m). Bioclastic content is reduced to microbioclastic detritus, occurring both in wackestones and in clasts of the breccia, suggesting its basinal provenance. This facies belt succeeded the lower slope facies.

The facies recognised enabled the reconstruction of the depositional architecture of a carbonate slope located in the eastern part of the Tulcea Unit, in North Dobrogea (Text-fig. 5). The facies architecture seems to have been influenced by sea-level changes and tectonic tilting.

During the early Middle Anisian (Bithynian), the carbonate platform underwent a change from toe-of-slope to lower slope, culminating in the upper slope. The entire stratigraphic succession ended with pelagic limestone. The observed facies changes suggest an initial transgressive trend (platform retrogradation), followed by progradation and platform drowning.

The depositional geometry of the upper slope built by microbial carbonates could not be determined in the field. It is inferred, however, that it was analogue to known examples, such as the Latemar platform in the Italian Dolomites (Marangon *et al.* 2011), the Siera del Cuera, in Spain, and some recent flat-topped systems (Della Porta *et al.* 2003). By analogy, the microbialites from the Middle Triassic of North Dobrogea could have extended on a steep slope to depths of ~200–300 m (Kenter *et al.* 2005).

DIAGENETIC HISTORY

The major diagenetic imprint on the slope and platform-margin Middle Triassic carbonates in the Mahmudia Quarry is their massive early marine cementation. Some carbonate platforms show this feature determined by the following factors: accommodation space, slow rates, low carbonate production, margin topography and effective fluid flow (Seeling *et al.* 2005). Brown fibrous cement, often appearing as thick isopachous crust, volumetrically dominates the coarser facies and as it

Samples	Texture/ Lithology	$\delta^{13}C$ (‰)	$\delta^{18}O$ (‰)
81	Micrite	3.58	-2.54
81	Micrite	2.80	-2.31
83	Micrite	1.88	-3.23
83	RFC	1.99	-5.45
87	Micrite	2.16	-4.19
94A	Micrite	3.06	-2.31
94A	Micrite	2.90	-2.69
113A	Micrite	3.61	-3.49
113A	Fibrous cement	3.40	-3.76
113A	Fibrous cement	3.70	-3.53
114D	Micrite	3.22	-3.50
114D	Late blocky calcite	2.45	-10.66
127A	Fibrous cement	3.59	-3.78
127A	*Tubiphytes*	3.78	-2.08
142B	Late blocky calcite	3.12	-3.79
142B	Micrite	3.72	-3.75

Table 2. Carbon and oxygen isotope composition of the lower Middle Anisian carbonates of the Caerace Formation in the Mahmudia Quarry, North Dobrogea

does not display any evidence of dissolution, is interpreted as penecontemporaneous cement deposited when the reef was in active contact with seawater (Payne *et al.* 2006). The second important cement type, occurring mostly in the boundstone facies, is the radiaxial fibrous calcite cement. Mm- to cm-thick isopachous crusts contain dark- and light-coloured bands, which show bright fluorescence and indicate several episodes of cementation, possibly biologically/microbially mediated. Fractures filled by several generations of cement interfingered with micritic laminae (Pl. 7, Fig. 5) suggest that cementation occurred while the voids were still open to marine waters prior to significant burial. These crusts have allowed the exceptional preservation of the abundant macroinvertebrate fossils in the lower Middle Anisian *Tubiphytes*-boundstones in the study area.

Syntaxial overgrowth cement on crinoidal fragments is a feature of the rudstone facies (Pl. 7, Fig. 6). Its cloudy appearance indicates that it was precipitated in the early stages of diagenesis. Blocky calcite is a minor component of the coarser facies, filling mostly the remaining cavities after precipitation of previous marine cements. In the cement-dominated boundstone facies large crystals of sparry calcite cannibalize the earlier fibrous marine cements as an effect of burial/ meteoric solutions (Pl. 7, Fig. 1; Pl. 8, Figs 1, 2). Some pores filled by blocky calcite exhibit luminescence of the crystals due to anoxic conditions at the depth where they were buried (Pl. 8, Fig. 3).

The $\delta^{13}C$ of cement samples is quite homogeneous (Table 2), varying between 1.88‰ and 3.78‰ (based on 32 analyses), whereas $\delta^{18}O$ values vary between -10.66‰ and -2.08‰. These data indicate that the carbonate cements precipitated from waters which became warm (Croquette and James 1987). Lower values are characteristic of blocky calcite in cements precipitated in the burial realm, associated with high temperatures and oxygen-depleted waters. The narrow range of $\delta^{13}C$ values can be explained by the fact that the samples were derived from a marine source and remained unchanged despite their transformations into diagenetic products (Peterhänsel and Egenhoff 2005). In Text-fig. 6 the isotopic data are grouped in a hypothetic trend of changing stable isotope composition, reflecting the diagenetic environments in which the cement and the other analysed carbonate sediments precipitated. In conclusion, the isotopic data indicate that most of the analysed samples were precipitated from solutions similar to marine Triassic waters (Korte *et al.* 2005).

As the paragenetic sequence (Text-fig. 7) reveals, carbonate diagenesis operated both in marine and burial environments, with a small meteoric vadose influence related to weathering surfaces. The time involved in diagenetic processes varies significantly in different diagenetic zones. Early diagenetic processes in shallow marine phreatic environments need less time than late diagenetic deeper burial diagenesis. Synsedimentary marine cements on platform slopes may grow over several tens of years resulting in synsedimentary stabilization of steep carbonate slope deposits (Grammer *et al.* 1993), while processes related to compaction during burial diagenesis can last millions of years.

Marine diagenesis dominates the slope sediments, expressed by massive marine cementation (Pl. 7, Figs 1–3, 5; Pl. 8, Figs 1, 6), incrustation/micritization of the clasts and selective dolomitization of the micritic clasts (Pl. 7, Fig. 6; Pl. 8, Fig. 7). Pelagic wackestones are also affected by matrix-selective dolomitization (Pl. 7, Figs 7, 8; Pl. 8, Fig. 5). Within the slope sediments pervasive replacement dolomite occurs mostly as a medium-crystalline, subhedral to euhedral planar mosaic, even the drusy cement being superimposed by dolomitization fronts (Pl. 8, Fig. 4). In some cases, the replacement of limestone by dolomite may generate an additional interparticle/intercrystal porosity, which, when supersaturated with respect to dolomite, will tend to form dolomite cements as overgrowths, so called ′dog-dooth cement′ (DTC, Pl. 7, Fig. 1; Pl. 8, Figs 1, 2). Penecontemporaneous dolomites form almost syndepositionally as a nor-

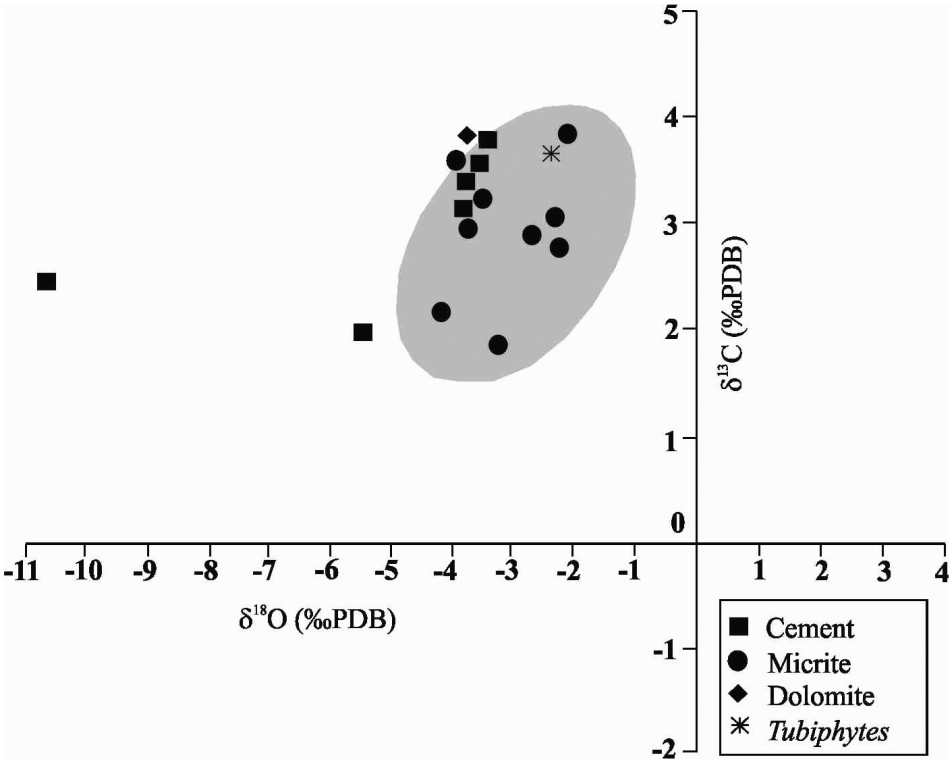

Text-fig. 6. Hypothetic trend of changing stable isotope composition in carbonate cement, micrite and dolomite, in the lower Middle Anisian section of the Caerace Formation. Isotopic composition of Triassic seawater based on data from brachiopod shells (Veizer *et al.* 1999; Korte *et al.* 2005) is indicated by the grey field

mal consequence of the geochemical conditions prevailing in the sedimentary environment (Machel 2004). The volumetrically large replacive dolostones associated with crinoidal floatstone facies (S6) (Pl. 5, Fig. 7; Pl. 6, Figs 1-3) are post-depositional and formed during burial. From various models of dolomitization, both reflux dolomitization and seawater dolomitization models are accepted herein. In the reflux model (Machel 2004), dolomitization is most commonly caused by mesohaline brines that originated from seawater evaporation during sea-level fluctuations, whereas seawater dolomitization is associated with post-depositional dolomites and diagenetic settings ranging in depth from shallow to intermediate burial. Beside other models having seawater in

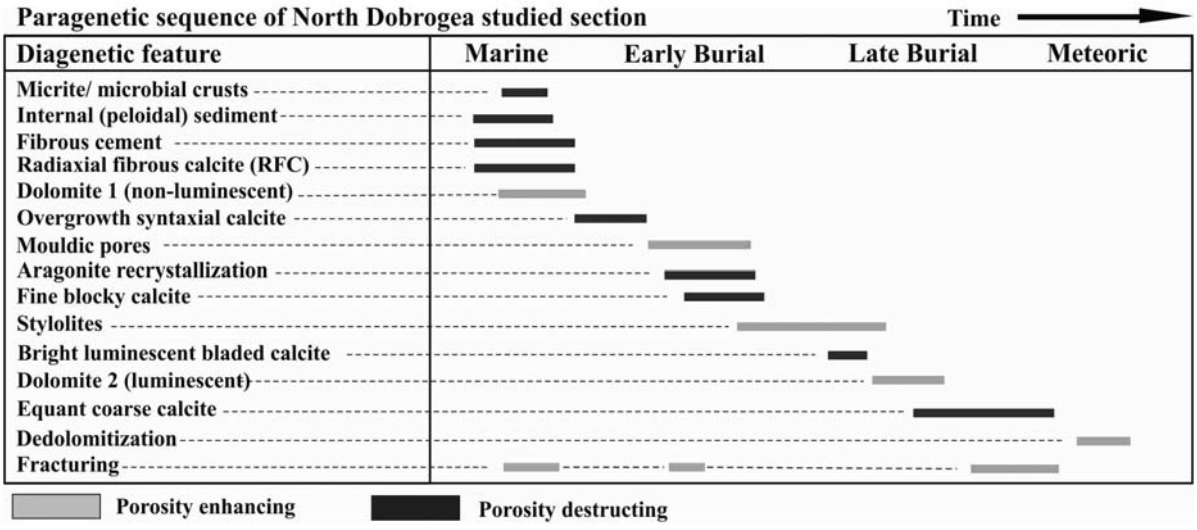

Text-fig. 7. Schematic representation of the diagenetic history of the lower Middle Anisian section of the Caerace Formation in the Mahmudia Quarry. Note the difference between porosity-destructing and porosity-enhancing factors

common as the main source of Mg, the seawater dolomitization model we adopted here comprises various possibilities of dolomitization by seawater.

Mouldic pores (Pl. 5, Figs 4, 7; Pl. 6, Figs 2, 3) and aragonite recrystallization (Pl. 6, Fig. 2), stylolites (Pl. 5, Fig. 6; Pl. 6, Figs 1, 3; Pl. 7, Fig. 7) and blocky calcite are common in the early burial stage. Dolomites cross-cut by stylolites (Pl. 6, Figs 1, 3; Pl. 7, Fig. 7) suggest burial of at least 600 m as stated by Machel (2004). The most common effect of late burial diagenesis is the appearance of microfractures filled by bright luminescent blocky calcite (Pl. 8, Fig. 3), the texture given by reducing fluids, and the second stage of dolomitization leading to an overgrowth of luminescent dolomite crystals over non-luminescent dolomite rims from pelagic facies, as revealed by cathodoluminescence (Pl. 8, Fig 5). The meteoric diagenesis includes de-dolomitization processes (Pl. 8, Fig. 8) caused by subaerial exposure of rocks and action of acid fluids.

COMPARISON WITH OTHER *TUBIPHYTES*-BUILDUPS KNOWN IN THE GEOLOGICAL RECORD

The Anisian represents the time of recovery of biogenic carbonate production after the crisis at the Permian/Triassic boundary (Gaetani *et al.* 1981; Senowbari-Daryan *et al.* 1993; Berra *et al.* 2005). In this context, the lower Middle Anisian section in Mahmudia Quarry is of particular importance in revealing the recovery of carbonate production during the Early Mesozoic. It documents the first record of a *Tubiphytes*-buildup in the North Dobrogean Orogen, similar to those known from Western and Eastern Tethys, characterized by the absence of metazoan reef communities and the dominance of micro-encrusters, automicrite and synsedimentary cements. As in other parts of the Tethys (Stanley 1988; Gaetani and Gorza 1989; Payne *et al.* 2006), the development of large, metazoan framework reefs in North Dobrogea started after the Anisian (Upper Ladinian–Carnian Wetterstein-type carbonate facies; see e.g. Grădinaru 1995, 2000).

The North Dobrogean *Tubiphytes*-dominated framework, with a high volume (30–50%) of penecontemporaneous and early-diagenetic cements and a considerable amount of automicrite, corresponds well to other *Tubiphytes*-dominated reefs, known from the Late Palaeozoic to Mesozoic: the Permian reefs of the Urals in Russia (Chuvashov 1983; Antoshkina 1998), the Permian Capitan Reef in the United States (Tinker 1998; Saller *et al.* 1999; Weidlich 2002), and the Middle Triassic (Anisian–Ladinian) reefs, such as the Great Bank of Guizhou, in south China (Enos *et al.* 1997, 2006; Lehrmann 1999; Payne *et al.* 2006, 2011; Lehrmann *et al.* 2007), the Camorelli Bank and Concarena platform in the Italian Lombardic Alps (Gaetani and Gorza 1989; Berra *et al.* 2005; Seeling *et al.* 2005), the Latemar platform in the Italian Dolomites (Harris 1993, 1994; Emmerich *et al.* 2005; Marangon *et al.* 2011; Preto *et al.* 2011), and the Aggtelek reef in Hungary (Velledits *et al.* 2011, 2012). Microbial boundstones, as *Tubiphytes*-dominated facies, are also the main constituents of the Carboniferous upper slopes in the Cantabrian Mountains in northern Spain (Della Porta *et al.* 2003; 2004; Kenter *et al.* 2005; Bahamonde *et al.* 2007).

Small Lower Triassic microbial reefs are known from the Caucasus, southern Germany, Iran and southern China (Flügel 2002). The Triassic recovery of the 'carbonate factory' is illustrated by the carbonate buildups that arose slowly during Anisian time and diversified considerably during the Ladinian. Most of the known Anisian reefs were located in the western part of the Tethys, between 10° and 20° N of the palaeo-equator, and are rare in its northern part (Text-fig. 8). Therefore the North Dobrogea location brings a new contribution to the Triassic reefs database. Alongside microbial-*Tubiphytes* boundstones in the Camorelli platform from Lombardy in northern Italy (Gaetani and Gorza 1989), small mounds in the Dont Formation of the Italian Dolomites (Blendinger 1983; Fois and Gaetani 1984), the carbonate mounds of Nakhlak in central Iran (Berra et al. 2012) and the Aggtelek reef in northeast Hungary (Velledits et al. 2011; 2012), the North Dobrogea *Tubiphytes*-buildup is probably among the oldest Tethyan Triassic bioconstructions.

Contrasting with other Anisian buildups, the amount of micritic sediment is not very high and a major role was played by synsedimentary marine cements. From this point of view, the lower Middle Anisian section in the Mahmudia Quarry resembles the shelf-edge framestones of the Anisian Chinese reefs (Enos *et al.* 1997, 2006; Payne *et al.* 2006) and the Middle Anisian to Lower Ladinian boundstone facies of Latemar (Harris 1993; Emmerich *et al.* 2005; Marangon *et al.* 2011) and Marmolada (Russo *et al.* 2000), both in the Italian Dolomites, and the Middle Anisian carbonate mounds in central Iran (Berra *et al*. 2012).

CONCLUDING REMARKS

The Middle Triassic carbonate platform in the eastern part of the Tulcea Unit, of the North Dobro-

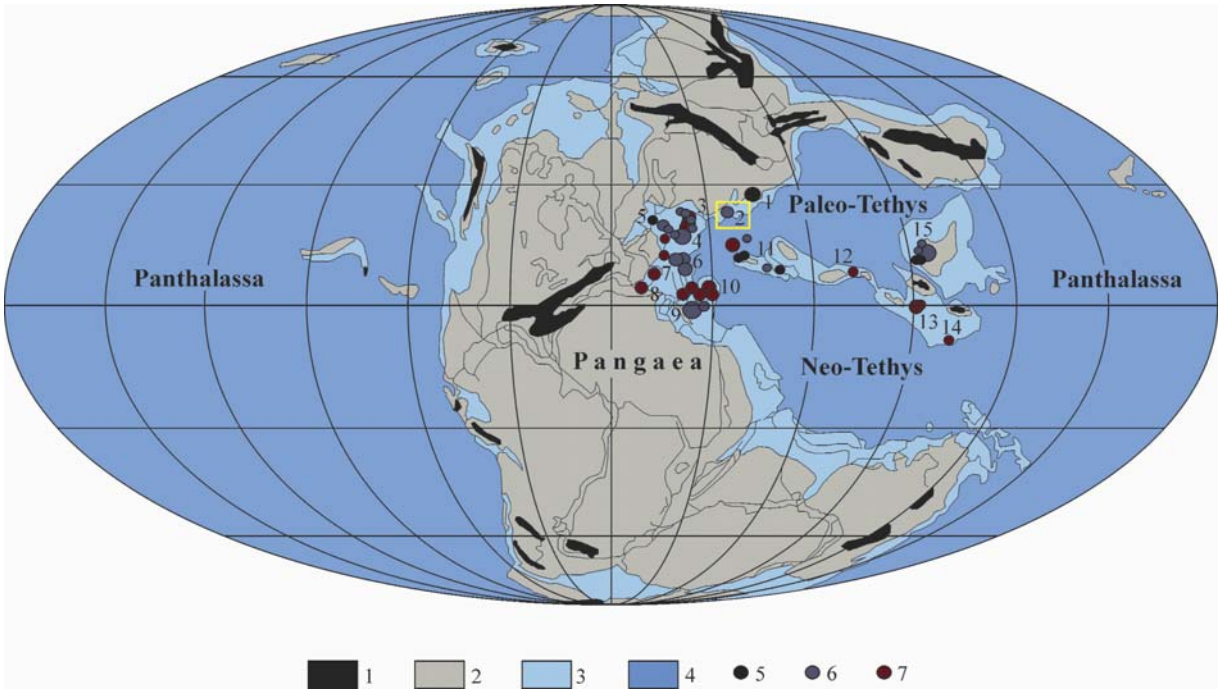

Text-fig. 8. Palaeogeographic map showing the distribution of Scythian to Ladinian reefs. Middle Triassic buildups are restricted to northern hemisphere, in the Western and Eastern Tethys (South China Plate), with the North Dobrogea Middle Anisian occurrence, in the northern part of the ocean. Legend: **1** – mountains; **2** – land; **3** – shelf; **4** – open ocean; **5** – Scythian microbial buildups; **6** – Anisian reefs; **7** – Ladinian reefs. Reef domains: **1** – Greater Caucasus, Russia; **2** – North Dobrogea, Romania (yellow box); **3** – Western Carpathians, Slovakia and northern Hungary; **4** – Northern Calcareous Alps, Austria and Bavaria; **5** – southern Germany; **6** – Southern Alps and Slovenia; **7** – northern Spain and southern France; **8** – southern Spain; **9** – southern Italy and former Yugoslavia; **10** – Carpathian Mountains, Romania; **11** – Iran; **12** – Pamir Mountains, Tadzhikistan; **13** – Thailand; **14** – Sumatra; **15** – southern China. Modified (completed) after Golonka and Kiessling (2012, personal communication) and Flügel (2002)

gean Orogen, in southeast Romania was studied. Facies analysis of a 200 m thick lower Middle Triassic carbonate sequence allowed the following conclusions:

Three facies belts of a carbonate slope, controlled by sea-level changes and tectonic tilting, were built at succeeding stages: (1) microbial-dominated upper slope stabilized by micro-encruster frameworks and large volumes of synsedimentary marine cements; (2) rudstones- and floatstones-dominated lower slope that represent precursor reef stages; and (3) toe-of-slope with basin influences indicated by pelagic wackestones.

The upper slope, dominated by high-rising microbialites, was self-nourishing and had no supply from the platform top.

The carbonate sequence from North Dobrogea compares well with other Carboniferous to Ladinian reefs, brings better understanding of the Triassic reefs and widens the knowledge of early Middle Triassic reefs throughout the Northern Tethys realm, which was considered a reef-free area during that time. The studied *Tubiphytes*-buildup from North Dobrogea is among the few lower Middle Anisian (Bithynian) reefs known from the Tethys, and represents the last "pure" M-type Triassic carbonate factory, before the transition toward a T-type factory, induced by the appearance of scleractinian corals.

Although after the Permian–Triassic extinction there was a crisis of reef building metazoans, it was not accompanied by a crisis in carbonate production. As the harsh climatic conditions that caused the extinction ameliorated, the early Anisian microbe-dominated buildups were replaced at the beginning of the Ladinian by sponge and scleractinian true reefs.

Acknowledgements

The first author would like to address special thanks to Prof. Jörn Peckmann and Dr. Tobias Himmler for generously providing stable isotope and SEM analysis, for valuable discussions and encouragements, during the guest-research period at MARUM Center (University of Bremen). We are indebted to the staff of Mahmudia Quarry SC-MIN-EST SA for

access and support, through the persons of Director-General Lorin Poiană, Eng. Geol. Adrian Tertiș and Eng. Valentin Pavel. Dr. Daniela Popescu and Dr. Liviu Popescu (University of Suceava) are kindly thanked for foraminiferal study, guidance in the manufacture of thin sections and for their hospitality. We kindly thank Mircea Vișan and Livius Popa for their company during fieldwork. We are indebted to Dr. Nereo Preto (Università di Padova) and Dr. Jonathan Payne (Stanford University) for discussions, useful comments and reviews that significantly improved the first version of the manuscript. Prof. Baba Senowbari-Daryan (Universität Erlangen-Nürnberg) is gratefully acknowledged for constructive comments and observations that improved the manuscript, mostly concerning the part that refers to the *Tubiphytes*-buildup. The thoughtful reviewing and valuable comments and suggestions by Prof. Maurizio Gaetani (Università degli Studi di Milano), Prof. Stanisław Skompski (University of Warsaw) and an anonymous referee that greatly contributed to the improvement of our paper are highly appreciated. Lastly, we are extremely grateful to the Editors, Prof. Ireneusz Walaszczyk and Christopher J. Wood, for their insightful reviewing and linguistic corrections.

The research was financially supported by POSDRU European Social Fund through the contract POSDRU/6/1.5/S/24, and by CNCSIS PNCDI-II-ID-1960/2009-2010.

REFERENCES

Antoshkina, A.I. 1998. Organic buildups and reefs on the Paleozoic carbonate platform margin, Pechora Urals, Russia. *Sedimentary Geology*, **118**, 187–211.

Bahamonde, J.R., Merino-Tomé, O.A. and Heredia, N. 2007. A Pennsylvanian microbial boundstone-dominated carbonate shelf in a distal foreland margin (Picos de Europa Province, NW Spain). *Sedimentary Geology*, **198**, 167–193.

Banks, C.J. and Robinson, A.G. 1997. Mesozoic Strike-Slip Back-Arc Basins of the Western Black Sea Region. In: Robinson, A.G. (Ed.), Regional and petroleum geology of the Black Sea and surrounding region. *AAPG Memoir*, **68**, 53–61.

Bebout, D.G. and Kerans, C. 1993. Guide to the Permian Reef Geology Trial, McKittrick Canyon, Guadalupe Mountains National Park, West Texas. Guidebook **26**, pp. 1–46. Bureau of Economic Geology, University of Texas.

Berra, F., Rettori, R. and Bassi, D. 2005. Recovery of carbonate platform production in the Lombardy Basin during the Anisian: paleoecological significance and constrain on paleogeographic evolution. *Facies*, **50** (3–4), 615–627.

Berra, F., Balini, M., Levera, M., Nicora, A. and Salamati, R. 2012. Anatomy of carbonate mounds from the Middle Anisian of Nakhlak (Central Iran): architecture and age of a subtidal microbial-bioclastic carbonate factory. *Facies*, **58**, 685–705.

Blendinger, W. 1983. Anisian sedimentation and tectonics of the M. Pore – M. Cernera area (Dolomites). *Rivista Italiana di Paleontologia e Stratigrafia,* **89**, 175–208.

Bucher, H. 1992. Ammonoids of the Hyatti Zone and the Anisian transgression in the Triassic Star Peak Group, northwestern Nevada, USA. *Palaeontographica*, **A 223**, 137–166.

Chuvashov, B.I. 1983. Permian Reefs of the Urals. *Facies*, **8** (1), 191–212.

Croquette, P.W. and Pray, L.C. 1970. Geologic nomenclature and classification of porosity in sedimentary carbonate rocks. *American Association of Petroleum Geologists Bulletin*, **54** (2), 207–250.

Croquette, P.W. and James, N.P. 1987. Diagenesis 12. Diagenesis in limestones 3. The deep burial environment. *Geoscience Canada*, **14**, 3–35.

Della Porta, G., Kenter, J.A.M., Bahamonde, J.R., Immenhauser, A. and Villa, E. 2003. Microbial Boundstones Dominated Carbonate Slope (Upper Carboniferous, N Spain): Microfacies, Lithofacies Distribution and Stratal Geometry. *Facies*, **49** (1), 175–208.

Della Porta, G., Kenter, J.A.M. and Bahamonde, J.R. 2004. Depositional facies and stratal geometry of an Upper Carboniferous prograding and aggrading high-relief carbonate platform (Cantabrian Mountains, N Spain). *Sedimentology*, **51**, 267–295.

Emmerich, A., Zamparelli, V., Bechstädt, T. and Zühlke, R. 2005. The reefal margin and slope of a Middle Triassic carbonate platform: the Latemar (Dolomites, Italy). *Facies*, **50** (3–4), 573–614.

Enos, P., Wei, J.I. and Yan, Y.J. 1997. Facies distribution and retreat of Middle Triassic platform margin, Guizhou Province, South China. *Sedimentology*, **44**, 563–584.

Enos, P., Lehrmann, D.J., Jiayong, W., Youyi, Y., Jiafei, X., Chaichin, D.H., Minzonni, M., Berri, A.C. and Montgomery, P. 2006. Triassic Evolution of the Yangtze Platform in Guizhou Province, People's Republic of China. *Geological Society of America, Special Paper,* **417**, 1–105.

Flügel, E. 1994. Pangean shelf carbonates: Controls and paleoclimatic significance of Permian and Triassic reefs. *Geological Society of America Special Papers*, **288**, 247–266.

Flügel, E. 2002. Triassic reef patterns. In: Kiessling, W., Flügel, E. and Golonka, J. (Eds), Phanerozoic reef patterns. *SEPM Special Publication*, **72**, 735–744. Tulsa.

Flügel, E. 2010. Microfacies of Carbonate Rocks, 2nd Edition, pp. 1–984. Springer; Berlin – Heidelberg.

Flügel, E. and Stanley, G.D. 1984. Reorganisation, development and evolution of post-Permian reefs and reef organisms. *Paleontographica Americana*, **54**, 177–186.

Fois, E. and Gaetani, M. 1984. The recovery of reef-building

communities and the role of cnidarians in carbonate sequences of the Middle Triassic (Anisian) in the Italian Dolomites. *Paleontographica Americana*, **54**, 191–200.

Gaetani, M., Fois, E., Jadoul, F. and Nicora, A. 1981. Nature and evolution of Middle Triassic carbonate buildups in the Dolomites (Italy). *Marine Geology*, **44** (1–2), 25–57.

Gaetani, M. and Gorza, M. 1989. The Anisian (Middle Triassic) carbonate bank of Camorelli (Lombardy, southern Alps). *Facies*, **21** (1), 41–56.

Grammer, G.M., Ginsburg, R.N., Swart, P.K., McNeil, D.F., Jull, A.J.T. and Prezbindowski, D.R. 1993. Rapid growth rates of syndepositional marine aragonite cements in steep marginal slope deposits, Bahamas and Belize. *Journal of Sedimentary Petrology*, **63** (5), 983–989.

Grădinaru, E. 1988. Jurassic sedimentary rocks and bimodal volcanics of the Cîrjelari-Camena Outcrop Belt: evidence for a transtensile regime of the Peceneaga-Camena Fault. *Studii și Cercetări de Geologie, Geofizică, Geografie, Seria Geologie*, **33**, 97–121.

Grădinaru, E. 1995. Mesozoic rocks in North Dobrogea: an overview. In: Săndulescu, M. and Grădinaru, E. (Eds), IGCP Project No. 369, Comparative Evolution of PeriTethyan Rift Basins. Central and North Dobrogea, Romania, October 1–4, 1995. *Field Guidebook*, pp. 17–28, Bucharest.

Grădinaru, E. 2000. Introduction to the Triassic Geology of North Dobrogea Orogene. In: Grădinaru, E. (Ed.), Workshop on the Lower-Middle Triassic (Olenekian-Anisian) boundary, 7–10 June 2000, Tulcea, Romania, Conference and Field Trip. Field Trip Guide, pp. 5–37, Bucharest.

Harris, M. T. 1993. Reef fabrics, biotic crusts and syndepositional cements of the Latemar reef margin (Middle Triassic), Northern Italy. *Sedimentology*, **40**, 383–401.

Harris, M.T. 1994. The foreslope and toe-of-slope facies of the Middle Triassic Latemar buildup (Dolomites, Northern Italy). *Journal of Sedimentary Research*, **64** (2), 132–145.

Kenter, J.A.M., Harris, P.M. and Della Porta, G. 2005. Steep microbial boundstone-dominated platform margins – examples and implications. *Sedimentary Geology*, **178**, 5–30.

Keim, L. and Schlager, W. 1999. Automicrite Facies on Steep Slopes (Triassic, Dolomites, Italy). *Facies*, **41** (1), 15–26.

Keim, L. and Schlager, W. 2001. Quantitative compositional analysis of a Triassic carbonate platform (Southern Alps, Italy). *Sedimentary Geology*, **139**, 261–283.

Kiessling, W. 2010. Reef expansion during the Triassic: Spread of photosymbiosis balancing climatic cooling. *Palaeogeography, Palaeoclimatology, Palaeoecology*, **290**, 11–19.

Kiessling, W., Flügel, E. and Golonka, J. 1999. Paleoreef maps: evaluation of a comprehension database on Phanerozoic reefs. *AAPG Bulletin*, **83**, 1552–1587.

Korte, C., Kozur, H. and Veizer, J. 2005. $\delta^{13}C$ and $\delta^{18}O$ values of Triassic brachiopods and carbonate rocks as proxies for coeval seawater and palaeotemperature. *Palaeogeography, Palaeoclimatology, Palaeoecology*, **226**, 287–306.

Lehrmann, D.J. 1999. Early Triassic calcimicrobial mounds and biostromes of the Nanpanjiang basin, south China. *Geology*, **27** (4), 359–362.

Lehrmann, D.J., Payne, J.L., Pei, D., Enos, P., Druke, D., Steffen, K., Zhang, J., Wei, J., Orchard, M. and Ellwood, B. 2007. Record of the end-Permian extinction and Triassic biotic recovery in the Chongzuo-Pingguo platform, southern Nanpanjiang basin, Guangxi, south China. *Palaeogeography, Palaeoclimatology, Palaeoecology*, **252**, 200–217.

Lighty, R.G. 1985. Preservation of internal reef porosity and diagenetic sealing of submerged early Holocene barrier reef, southeast Florida shelf. *SEPM Special Publication*, **36**, 123–152. Tulsa.

Machel, H.G. 2004. Concepts and models of dolomitization: a critical reappraisal. In: Braithwaite, C.J.R., Rizzi, G. and Darke, G. (Eds), The Geometry and Petrogenesis of Dolomite Hydrocarbon Reservoirs. *Geological Society, London, Special Publications*, **235**, 7–63.

Marangon, A., Gattolin, G., Della Porta, G. and Preto, N. 2011. The Latemar: A flat-topped, steep fronted platform dominated by microbialites and synsedimentary cements. *Sedimentary Geology*, **240**, 97–114.

Mietto, P. and Manfrin, S. 1995. A high resolution Middle Triassic ammonoid standard scale in the Tethys Realm. A preliminary report. *Bulletin de la Société Géologique de France*, **166** (5), 539–563.

Mirăuță, E. and Panin, N. 1976. Geological Map of Romania, Scale 1:50,000, Sheet 136c Mahmudia, Institute of Geology and Geophysics, Bucharest.

Monnet, C. and Bucher, H. 2006. Anisian (Middle Triassic) ammonoids from North America: quantitative biochronology and biodiversity. *Stratigraphy*, **2** (4), 281–296.

Mundy, D.J.C. 1994. Microbialite-sponge-bryozoan-coral framestones in Lower Carboniferous (late Visean) buildups of northern England (UK). In: Embry, A.F., Beauchamp, B. and Glass, D.J. (Eds), Pangea: Global Environments and Resources. *Canadian Society of Petroleum Geologists, Memoir*, **17**, 713–729.

Okay, A.I., Şengör, A.M.C. and Görür, N. 1994. Kinematic history of the opening of the Black Sea and its effect on the surrounding regions. *Geology*, **22** (3), 267–270.

Payne, J.L., Lehrmann, D.J., Christensen, S., Wei, J. and Knoll, A.H. 2006. Environmental and biological controls on the initiation and growth of a Middle Triassic (Anisian) Reef Complex on the Great Bank of Guizhou, Guizhou Province, China. *Palaios*, **21**, 325–343.

Payne, J.L., Summers, M., Rego, B.L., Altiner, D., Wei, J., Yu, M. and Lehrmann, D.J. 2011. Early and Middle Triassic

trends in diversity, evenness, and size of foraminifers on a carbonate platform in south China: implications for tempo and mode of biotic recovery from the end-Permian mass extinction. *Paleobiology*, **37** (3), 409–425.

Peterhänsel, A. and Egenhoff, S.O. 2005. Sea level changes versus hydrothermal diagenesis: Origin of Triassic carbonate platform cycles in the Dolomites, Italy: Discussion. *Sedimentary Geology*, **178**, 145–149.

Playford, P.E., Hurley, N.F., Kerans, C. and Middleton, M. 1989. Reefal platform development, Devonian of the Canning Basin, Western Australia. In: Crevello, P.D., Wilson, J.L., Sarg, J.F. and Read, J.F. (Eds): Controls on carbonate platforms and basin development. *SEPM Special Publication,* **44**, 187–202. Tulsa.

Pratt, B.R. 1995. The origin, biota and evolution of deep-water mud-mounds. In: Monty, C.L.V., Bosence, D.W.J., Bridges, P.H. and Pratt, B.R. (Eds): Carbonate Mud-Mounds. Their Origin and Evolution. *Special Publication of the International Association of Sedimentologists Series*, **23,** pp. 49–123. Wiley-Blackwell.

Preto, N., Kustatscher, E. and Wignall, P.B. 2010. Triassic climates – State of art and perspectives. *Palaeogeography, Palaeoclimatology, Palaeoecology*, **290**, 1–10.

Preto, N., Franceschi, M., Gattolin, G., Massironi, M., Riva, A., Gramigna, P., Bertoldi, L. and Nardon, S. 2011. The Latemar: A Middle Triassic polygonal fault-block platform controlled by synsedimentary tectonics. *Sedimentary Geology*, **234**, 1–18.

Riding, R. and Guo, L. 1992. Affinities of *Tubiphytes*. *Palaeontology*, **35** (1), 37–49.

Rollins, H.B. and Donahue, J. 1975. Towards a theoretical basis of paleoecology: concepts of community developments. *Lethaia*, **8**, 255–270.

Russo, F., Mastandrea, A., Stefani, M. and Neri, C. 2000. Carbonate facies dominated by syndepositional cements: a key component of Middle Triassic platforms. The Marmolada case history (Dolomites, Italy). *Facies*, **42** (1), 211–226.

Saller, A.H., Harris, P.M., Kirkland, B.L. and Mazzullo, S.J. 1999. Geologic Framework of the Capitan Reef. *SEPM Special Publication*, **65**, pp. 1–224.

Săndulescu, M. 1995. Dobrogea within the Carpathian Foreland. In: Săndulescu, M. and Grădinaru, E. (Eds), IGCP Project No. 369, Comparative Evolution of PeriTethyan Rift Basins. Central and North Dobrogea, Romania, October 1–4, 1995. Field Guidebook, pp. 1–4, Bucharest.

Schlager, W. 2000. Sedimentation rates and growth potential of tropical, cool-water and mud-mound carbonate factories. In: Insalaco, E., Skelton, P.W., Palmer, T.J. (Eds), Carbonate platform systems: components and interactions. *Geological Society, London, Special Publication*, **178**, 217–227.

Schlager, W. 2003. Benthic carbonate factories of the Phanerozoic. *International Journal of Earth Sciences*, **92** (4), 445–464.

Seeling, M., Emmerich, A., Bechstädt, T. and Zühlke, R. 2005. Accomodation/sedimentation development and massive early marine cementation: Latemar vs. Concarena (Middle/Upper Triassic, Southern Alps). *Sedimentary Geology*, **175**, 439–457.

Senowbari-Daryan, B. 2013. *Tubiphytes* Maslov, 1956 and description of similar organisms from Triassic reefs of the Tethys. *Facies*, **59**, 75–112.

Senowbari-Daryan, B., Zühlke, R., Bechstädt, T. and Flügel, E. 1993. Anisian (Middle Triassic) Buildups of the Northern Dolomites (Italy): The Recovery of the Reef Communities after the Permian/ Triassic Crisis. *Facies*, **28** (1), 181–256.

Senowbari-Daryan, B., Bucur, I.I., Schlagintweit, F., Săsăran, E. and Matyszkiewicz, J. 2008. *Crescentinella*, a new name for "*Tubiphytes*" *morronensis* Crescenti, 1969: an enigmatic Jurassic-Cretaceous microfossil. *Geologica Croatica*, **61** (2–3), 185–214.

Şengör, A.M.C. 1984. The Cimmeride Orogenic System and the Tectonics of Eurasia. *Geological Society of America, Special Paper*, **195**, IX + 82 pp.

Şengör, A.M.C. 1986. Die Alpiden und die Kimmeriden: die verdoppelte Geschichte der Tethys. *Geologische Rundschau*, **75**, 501–510.

Shen, J., Yu, C. and Bao, H. 1997. A Late Devonian (Famennian) *Renalcis-Epiphyton* reef at Zhaijiang, Guilin, South China. *Facies*, **37** (1), 95–210.

Shevyrev, A.A. 1990. Ammonoids and chronostratigraphy of the Triassic. pp. 1–179. Nauka, Moscow. [In Russian]

Shevyrev, A.A. 1995. Triassic ammonites of northwestern Caucasus, pp. 1–174. Nauka, Moscow. [In Russian]

Silberling, N.J. and Nichols, K.M. 1982. Middle Triassic Molluscan Fossils of Biostratigraphic Significance from the Humboldt Range, Northwestern Nevada. *Geological Survey Professional Paper* **1207**, V + 77 pp.

Stanley, G.D. 1988. The History of Early Mesozoic reef communities: A three-step process. *Palaios*, **3**, 170–183.

Stefani, M., Furin, S. and Gianolla, P. 2010. The changing climate framework and depositional dynamics of Triassic carbonate platforms from the Dolomites. *Palaeogeography, Palaeoclimatology, Palaeoecology*, **290**, 43–57.

Tinker, S.W. 1998. Shelf-to-basin facies distributions and sequence stratigraphy of a steep-rimmed carbonate margin: Capitan depositional system, McKittrick Canyon, New Mexico and Texas. *Journal of Sedimentary Research*, **68** (6), 1146–1174.

Veizer, J., Ala, D., Azmy, K., Bruckschen, P., Buhl, D., Bruhn, F., Carden, G.A.F., Diener, A., Ebneth, S., Godderis, Y., Jasper, T., Korte, C., Pawellek, F., Podlaha, O.G. and Strass, H. 1999. $^{87}Sr/^{86}Sr$, $\delta^{13}C$, and $\delta^{18}O$ evolution of

Phanerozoic seawater. *Chemical Geology*, **161**, 59–88.

Velledits, F., Péró, C., Blau, J., Senowbari-Daryan, B., Kovács, S., Piros, O., Pocsai, T., Szügyi-Simon, H., Dumitrică, P. and Pálfi, J. 2011. The oldest Triassic platform margin reef from the Alpine-Carpathian region (Aggtelek, NE Hungary): platform evolution, reefal biota and biostratigraphic framework. *Rivista Italiana di Paleontologia e Stratigrafia*, **117** (2), 221–268.

Velledits, F., Hips, K. and Péró, C. 2012. Lower and Middle Triassic succession in Aggtelek Karst. IGCP 572 field trip POST 2. June 5–7, 2012. 1–33.

Visarion, M., Săndulescu, M., Roșca, V., Stănică, D., and Atanasiu, L. 1990. La Dobrogea dans le cadre de l'avant pays carpatique. *Revue Roumaine de Géophysique*, **34**, 55–65.

Webb, G.E. 1996. Was Phanerozoic reef history controlled by the distribution of non-enzymatically secreted reef carbonates (microbial carbonate and biologically induced cement)? *Sedimentology*, **43**, 947–971.

Weidlich, O. 2002. Middle and Late Permian reefs - distributional patterns and reservoir potential. In: Kiessling, W., Flügel, E. and Golonka, J. (Eds), Phanerozoic Reef Patterns. *SEPM Special Publication*, **72**, 339–390. Tulsa.

Wood, R. 1999. Reef evolution, 354 p. Oxford University Press; Oxford.

Wood, R. 2000. Novel paleoecology of a postextinction reef: Famennian (Late Devonian) of the Canning basin, northwestern Australia. *Geology*, **28** (11), 987–990.

Wood, R. 2001. Are reefs and mud mounds really so different? *Sedimentary Geology*, **145**, 161–171.

Manuscript submitted: 20th August 2013
Revised version accepted: 15th May 2014

PLATES 1–8

PLATE 1

1 – Outcrop of massive *Tubiphytes* boundstone (S1); the person in the left lower corner of the photo, the first author of this paper, as a scale.

2 – Hand specimen revealing early marine cement crusts (RFC) and *Tubiphytes* (T) micro-encrusters (S1).

3 – Detail of cm-sized cement crusts consisting of RFC and blocky calcite (bc) covering *Tubiphytes* boundstone (S1). [Photo taken under binocular lens and polarizing microscope]

4 – 'Grass-like' aggregate of branching individuals of *Tubiphytes* (T) reinforced by marine cement (S1).

5 – *Tubiphytes* (T) encrusted by foraminifers, forming an organic framework that also acted as a baffler; constructional cavities filled with internal sediment (is) that contains ostracods (o) and peloids (p), and fibrous cement (F). Inset, detail of internal sediment (is) with bacterial/microbial filaments (arrow) (S1, 125).

Note: Symbols S1 to S8, written under brackets in all 8 plates, refer to the lithofacies types listed in Table 1 (S1 – *Tubiphytes* boundstone; S2 – Bivalve coquina with automicrite; S3 – Cement-dominated boundstone; S4 – Bioclastic rudstone; S5 – Laminated bindstone; S6 – Crinoidal floatstone; S7 – Intraclast breccia; S8 – Pelagic wackestone), followed by the sample numbers in the lithostratigraphic log from Text-fig. 4.

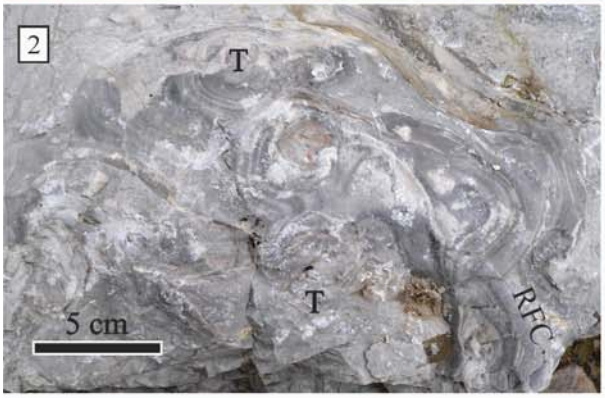

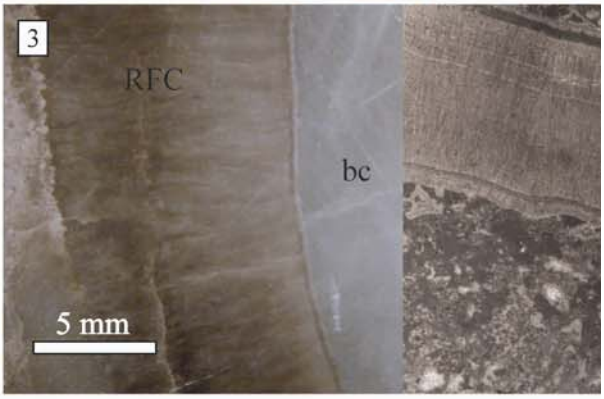

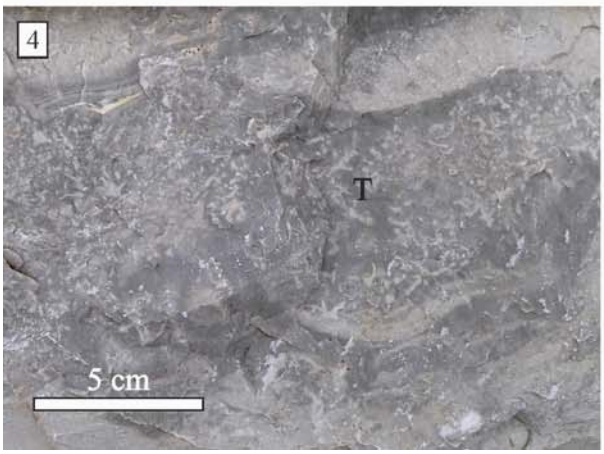

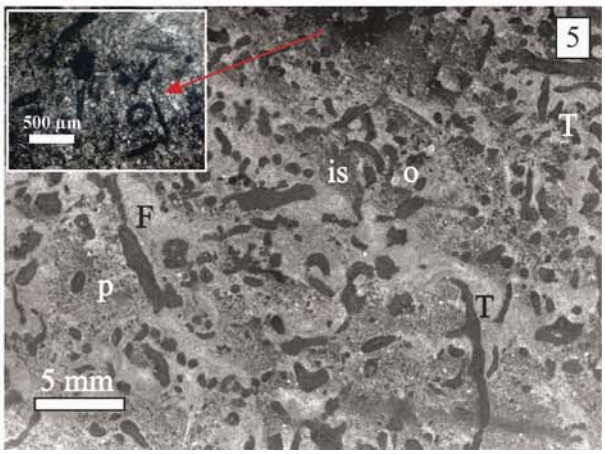

PLATE 2

1 – *Tubiphytes* (T) as digitate, micritic, vaguely laminated skeletons; three generations of cements (fibrous-F, RFC and blocky-bc) and internal sediment (is) fill voids generated by growth of *Tubiphytes*; black arrows indicate the biotic gravity-defying crusts and red arrows, foraminiferal tubes encrusting *Tubiphytes*; Inset, cross section through a *Tubiphytes* clast with a sessile foraminifer (f) test inside (S1, 127).

2 – *Tubiphytes* boundstone with high frequency of bioclasts: brachiopod (br), gastropod (g), bivalve (b) and *Tubiphytes* (T) (S1, 110A).

3 – Detail of boundstone facies: *Tubiphytes* clasts (T), ostracods (o) and foraminifera (f, *Textularia* sp.) embedded in fibrous calcite (F) and blocky calcite (bc); patches of automicrite (am) below to the right (S1, 138B).

4 – Longitudinal section through a *Tubiphytes* (T) specimen with the central sparitic tube (white arrows) embedded in a clotted micrite mass; foraminiferal encrustation below to the left left (black arrow); bivalve fragment (b) and automicrite (am); fibrous calcite (S1; 138B).

5 – Longitudinal-oblique section through a *Tubiphytes* (T) specimen with the sparitic tube surrounded by a thick laminated cortex with distinct growth stages of differing contrast and structure; encrusting foraminiferal tube (red arrow); irregular peloids (p) included in automicrite (am) patches; ostracod bioclasts (o) (S1, 127).

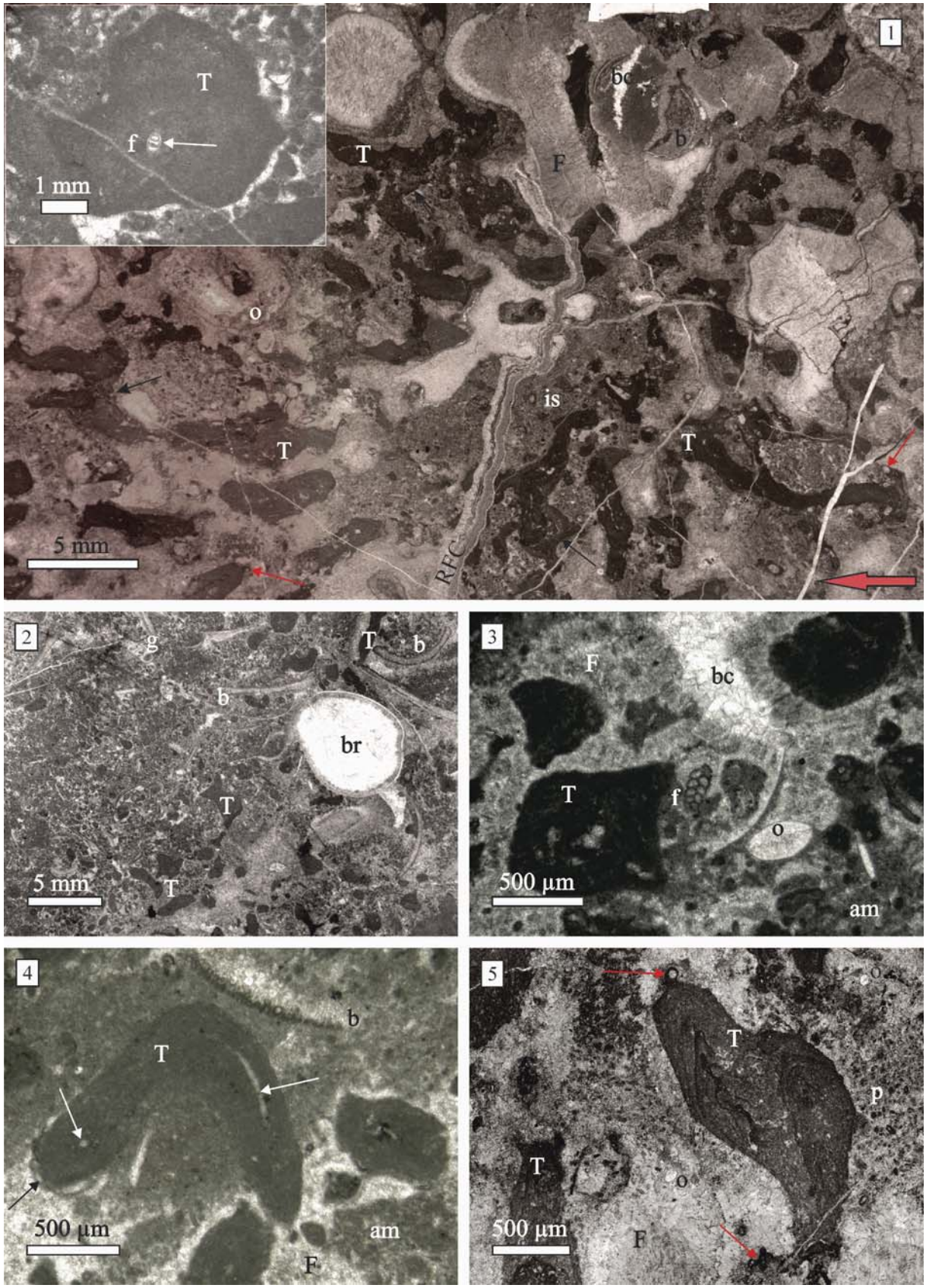

PLATE 3

1 – Geopetal structure infilling a bioturbation (bt) with a small brachiopod (br) caught in micritic sediment while the top of the cavity is blocky-cemented (bc); automicrite (am) patches and thin-shelled bivalves (b) embedded in fibrous cement (S1, 130.1).
2 – Boundstone with *Tubiphytes* specimens (T) caught in fibrous cement (F); porous spaces occluded by blocky calcite (bc) during burial; automicrite (am) (S1, 135B).
3 – Coquinite thin laminae (up to 5 cm thick) of recrystallized bivalve (b), gastropod (g), brachiopod (br) and ammonoid (A) shells filled by internal sediment and cemented by fibrous calcite; patches of automicrite (am) (S2, 104).
4 – Bivalve coquina with recrystallized shells (b) embedded in fibrous cement (F); automicrite (am), ostracods (o) and foraminifera (f) (S2, 115).
5 – Bivalve coquina with shells (b) intensively encrusted (arrows) and fibrous cement (F); T – *Tubiphytes* clast (S2, 139D).
6 – Bivalve coquina with geopetal structure (arrow) due to the infill of the bivalve shells (b); automicrite (am) with ostracods (o) (S2, 112).
7 – Cement boundstone dominated by microbial textures, with 'black and white' peloids (b&w p), *Muranella* spongiostromate microproblematic products (M?), and fibrous cementation (F) occluding the intraparticle porosity (S3, 113A).
8 – Detail for the peloids in Fig. 7 (black quadrant), with LMC centres and dolomitized rims (black arrows).

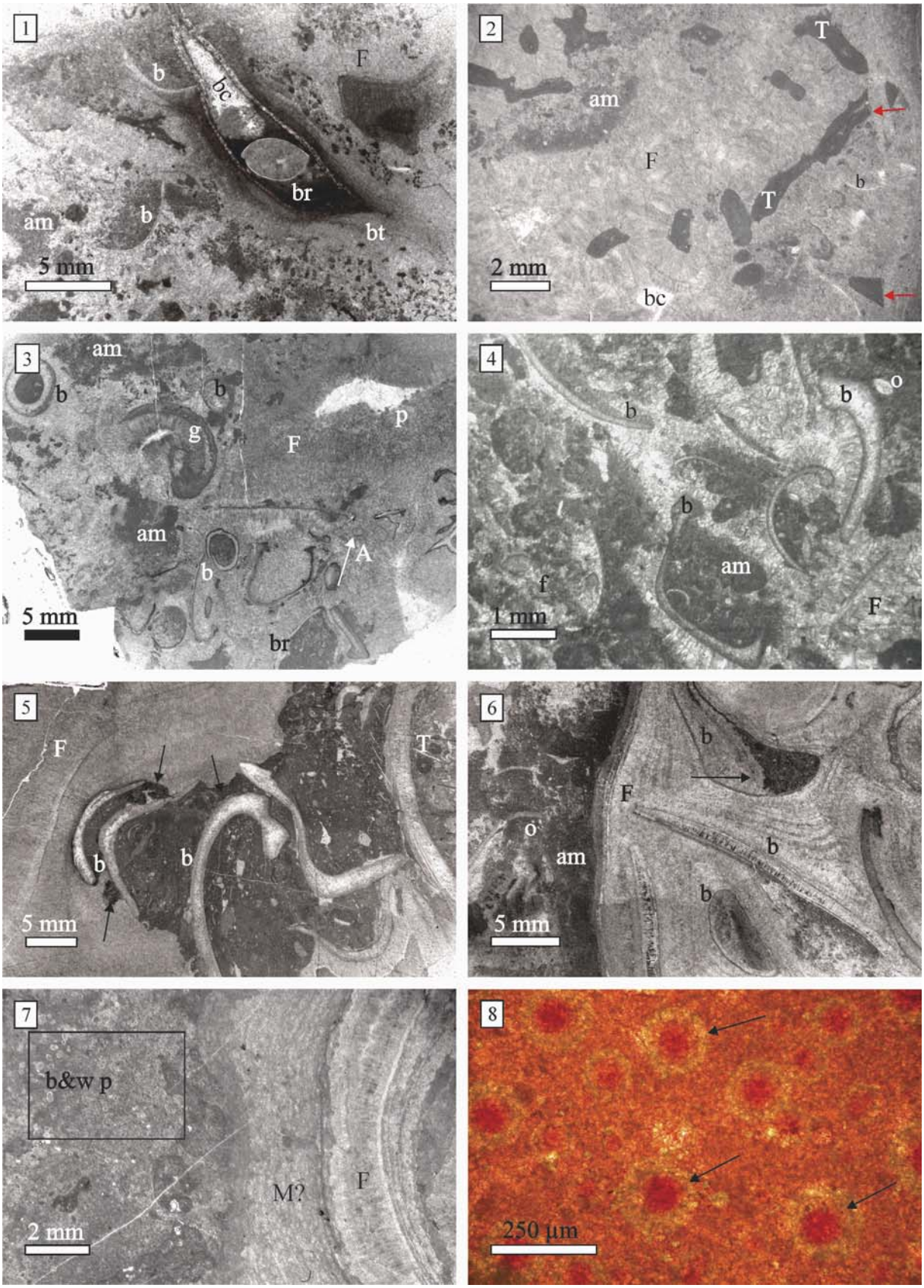

PLATE 4

1 – Microphotograph collage over a stained thin section in a bioclastic rudstone dominated by bioclast fragments (echinoderm, e; *Tubiphytes*, T) interfingering with laminated mudstones of thick peloid layers (p) that alternate with thin micrite films (m); patches of automicrite (am) intermingled with *Tubiphytes* (T) appearances. Several veins, crossing both textures, are peneconteporaneous with sedimentation, micrite laminae and intraclasts (i) being incorporated by the RFC that fill the veins (S4, 69).

2 – Inset 1 in Fig. 1, with *Tubiphytes* (T) clasts embedded in fibrous cement (F), large crinoid columnal (e), ostracod (o), peloids (p) and a fissure filled by RFC and micrite (m).

3 – Inset 2 in Fig. 1, with bioclasts (foraminifers, f, *Tubiphytes*, T), fibrous cement (F) and micrite lamina (m).

4 – Inset 3 in Fig. 1, with large fragments of echinoderms (e) and bivalves (b) surrounded by microbial encrustations (red arrows); a *Tubiphytes* (T) fragment with clearly visible sparite centre and RFC.

5 – Crinoid columnal (e) with honeycomb microtexture encrusted by *Tubiphytes* (T), in their turn with foraminiferal encrustations on peripheral areas (arrows) (S4, 69).

6 – Bioclastic rudstone transition (arrow) to laminated, fine-grained agglutinated stromatolite texture shown by alternation of irregular peloid (p) and micrite (m) laminae; *Tubiphytes* clasts (T), echinoderm (e), foraminifer (f), dasycladacean algae (a) and intraclasts (i) are cemented by fibrous calcite (S4 to S5 transition, 82).

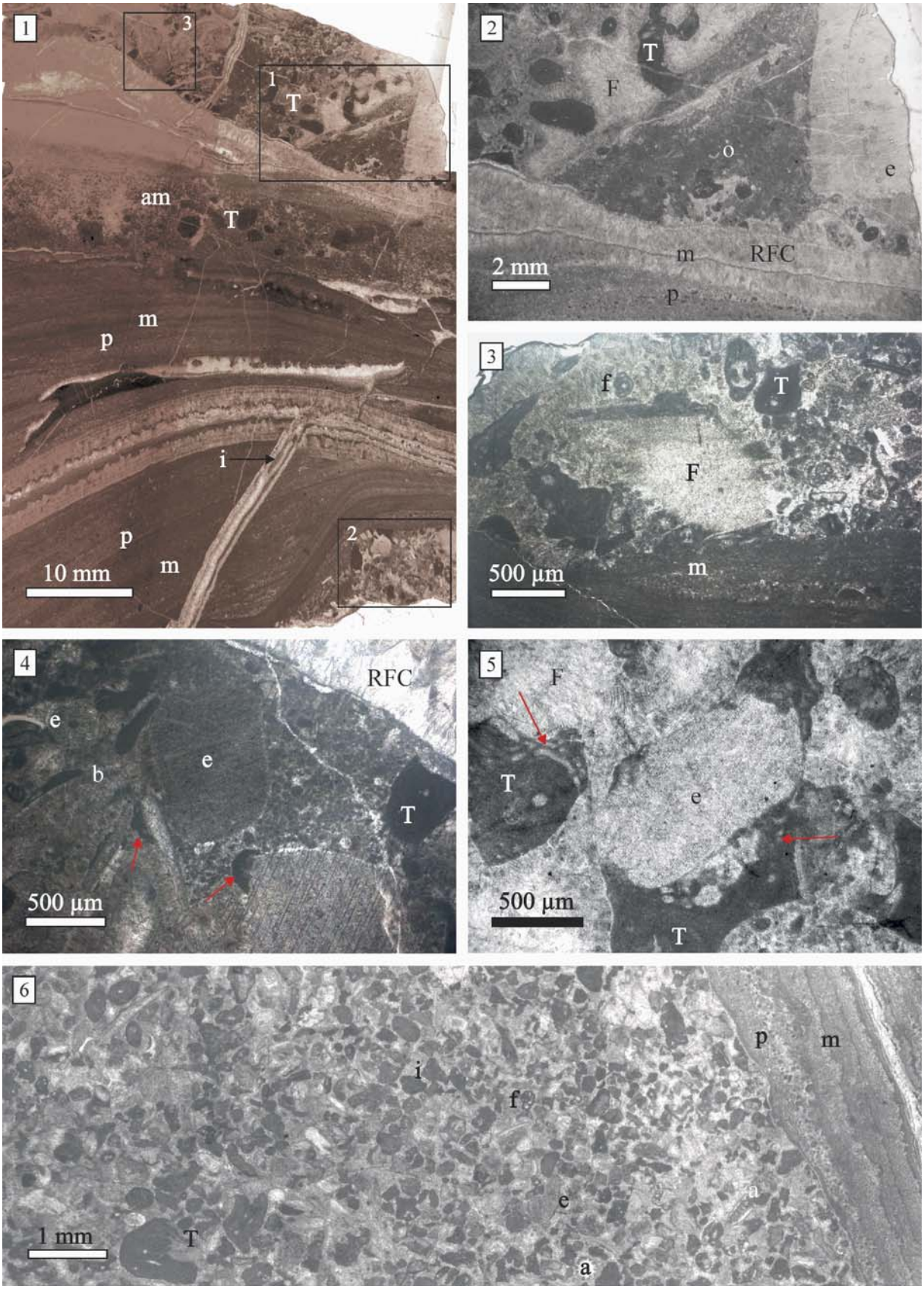

PLATE 5

1 – Bioclastic rudstone with bryozoan (bz), algae (a), echinoderm (e) and bivalve (b) fragments embedded in fibrous cement and blocky calcite (bc); soft dolomitized intraclasts (i) suggesting instability of the environment (S4, 83).

2 – Microphotograph with gastropod (g), echinoderm (e), bivalve (b), *Tubiphytes* (T) fragments, intraclasts (i), foraminifers (f) and bryozoans (bz); interparticle porosity occluded by fibrous and late blocky cement; most of the bioclasts are encrusted (arrow) (S4, 83).

3 – Bioclastic rudstone with foraminiferal encrustations of *Tolypammina gregaria* Wendt (black arrows), attached to a gastropod shell (g) and to *Tubiphytes* (T) (S4, 84).

4 – Gastropod shell with a mouldic porosity caused by aragonite dissolution and occluded by fibrous (F) and blocky calcite (bc) cement; foraminifers (*Geinitzina tcherdynzevi* Miklukho-Maklay) (red arrow), and clasts of *Tubiphytes* (T) (S4, 84).

5 – Interfingering of pelagic wackestone, with radiolarians (r) and micrite (m), and large isopachous cement crusts that incorporate large intraclasts, I (S6, S7, 87A).

6 – Laminated bindstone (geopetal infilling?) of fine-grained laminated peloidal grainstone grading into peloidal packstone; alternations of thicker peloid (p) and thin micrite (m) layers separated by irregular, probably microbial, micrite lamina (S5, 98C).

7 – Crinoidal floatstone with crinoid stem plates (e) and a large columnal, recrystallised brachiopod (br) and gastropods (g) in a dolomitized matrix (inset, detail by staining); microbial (?) encrustation of echinoderms (arrows), geopetal infilling of a gastropod shell in the left part of the photo (S6, 87).

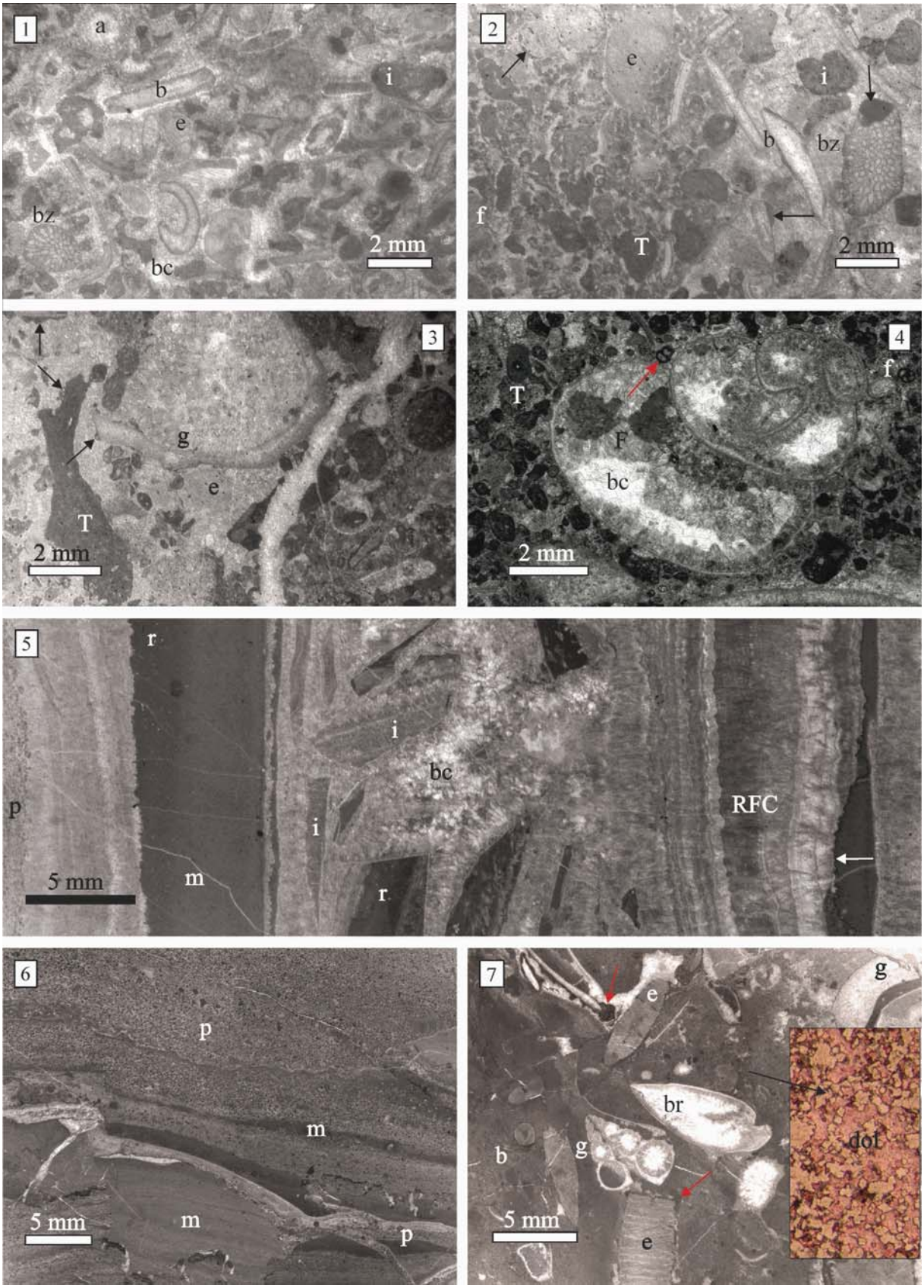

PLATE 6

1 – Scanned peel for the S2 - bivalve coquina microfacies with juvenile ammonoid shells (A) into a dolo-matrix together with echinoderm (e) fragments, thin-shelled bivalves and brachiopod (br); staining evidences the transformation of ammonoid aragonitic shell into LMC, respectively dolomite (arrow); a planar stylolite seen on the left-hand side (S6, 87).

2 – Crinoidal floatstone microfacies dominated by biogenic overgrowths created probably by foraminifera and microbes; crinoids columnals (e) with "honeycomb" microtexture and bivalve fragments (b) coated by microbial crusts; foraminiferal oncoids (arrows) made by long-lasting encrustations; saucer-shaped bivalve shells displaying a geopetal feature; ammonoid fragment (A) with partly recrystallised shell, and partly filled by sediment. (S6, 87).

3 – Composite photomicrograph in a crinoidal floatstone; echinoderm fragments (e), gastropod shells (g), fragments of punctate brachiopods (br) embedded in a muddy matrix crossed by numerous peloid bands (p); dolomitized intraclast (i) rimmed by fibrous calcite showing a soft texture (S6, 86).

4 – Detail of the outcrop showing the irregular (erosional?) contact between bioclastic rudstone (S4), intraclast breccia (S7) and burrowed pelagic wackestone (S8).

5 – Intraclast breccia with clasts and matrix (m) of pelagic microbioclastic wackestone; calcified radiolarians (r), sessile foraminifers (f), sponge spicules (s) and thin-shelled bivalves (b) suggesting a deeper-water environment, within a slope setting (S7, 91).

6 – Burrowed pelagic wackestone microfacies with pelagic detritus, recrystallized radiolarians (r), thin-shelled bivalves (b), uniserial foraminifers (f) and sponge spicules (s) embedded in muddy matrix; bioturbations (bt) as dark patches (S8, 94).

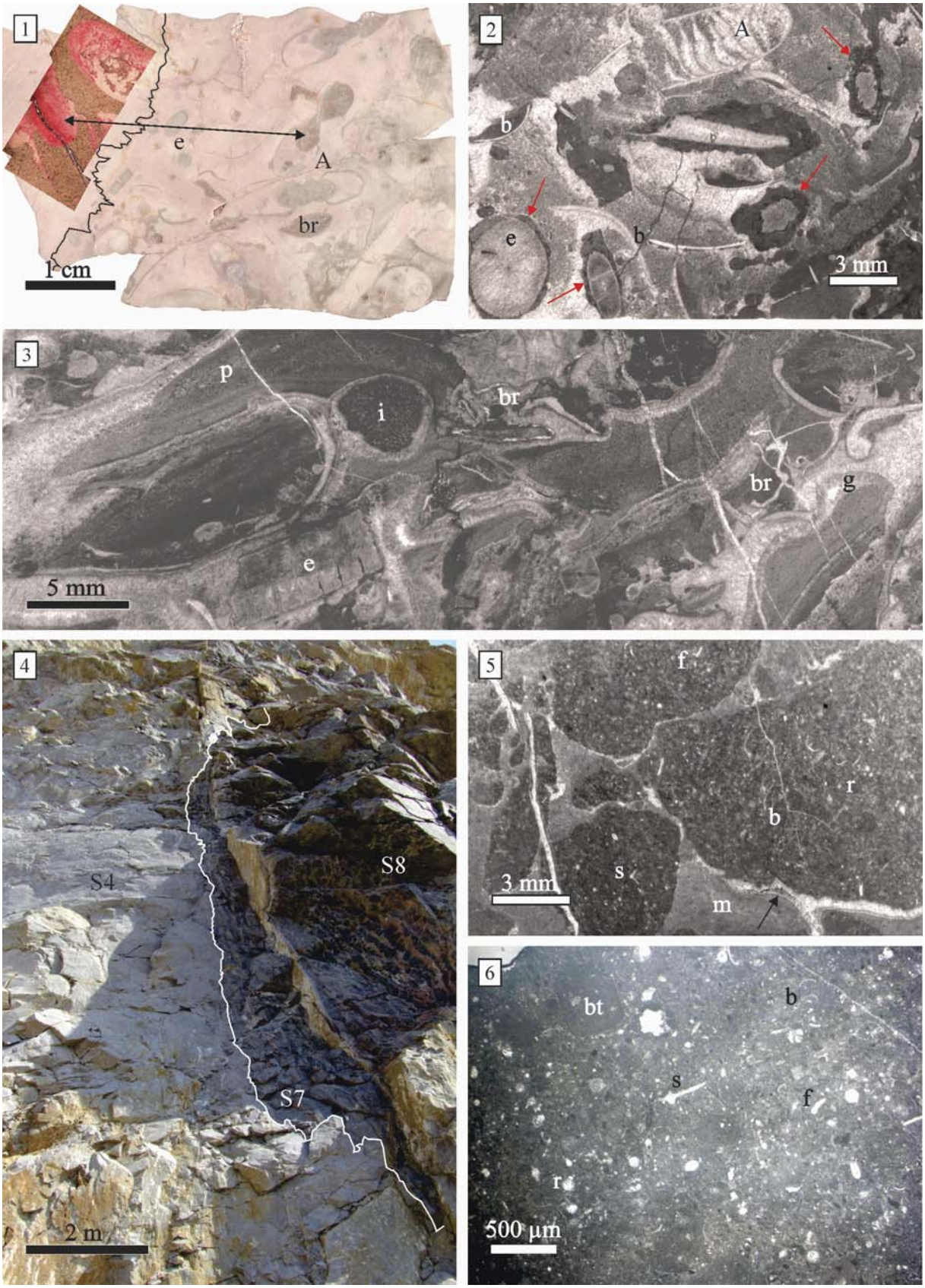

PLATE 7

1 – Composite photomicrograph of cement-dominated boundstone; fibrous cement (F) and 'dog-tooth' dolomite cement – DTC (stained white) rimming pore walls and late blocky calcite (bc) cannibalizing previous phases. Patches of automicrite (am) detailed in the next photo (S3, 114D).

2 – Thrombolitic fabric of automicrite (am) with peloidal aggregates within fibrous cement (F); wavy cement layers shown by a distinct growth structure probably of organic mats (S3, 114D).

3 – Dewatering structures (arrows) and soft sediment of dark- and light-coloured micritic laminae (m), indicating slope conditions. Large amounts of fibrous cement (F) proving that good water circulation favoured the cementation (S3, 142A).

4 – Stromatactis structures (black arrow) showing a flat floor garnished with peloids and digitate roof; RFC lines the walls of cavities, while blocky calcite (bc) fills the remaining space; another pore filled by blocky calcite; dolomitized clasts of *Tubiphytes* (T) and patches of automicrite (am). The red arrow indicates the top of the sediment (S3, 142B).

5 – Contemporaneous veins filled by several generations of carbonate cement: fibrous isopachous crust (ic), RFC and late blocky calcite (bc); thin layers of micrite (m) and intraclasts (i) suggesting Neptunian origin (S4, 69).

6 – Syntaxial overgrowths (so) on crinoidal plates (e), with a single-crystal appearance; soft dolomitized intraclasts (i) and blocky calcite (bc) fill the remaining space (S4, 81).

7 – Stylolite rimmed by clay residue (dark coloured) separates poorly dolomitized micritic matrix (m) from dolomitized sediment (dol), as revealed by staining. (S8, 93A).

8 – Dolomite rhombic crystals (dol) enclosed in a matrix of equigranular microcrystallized calcite (SEM image) (S8, 94).

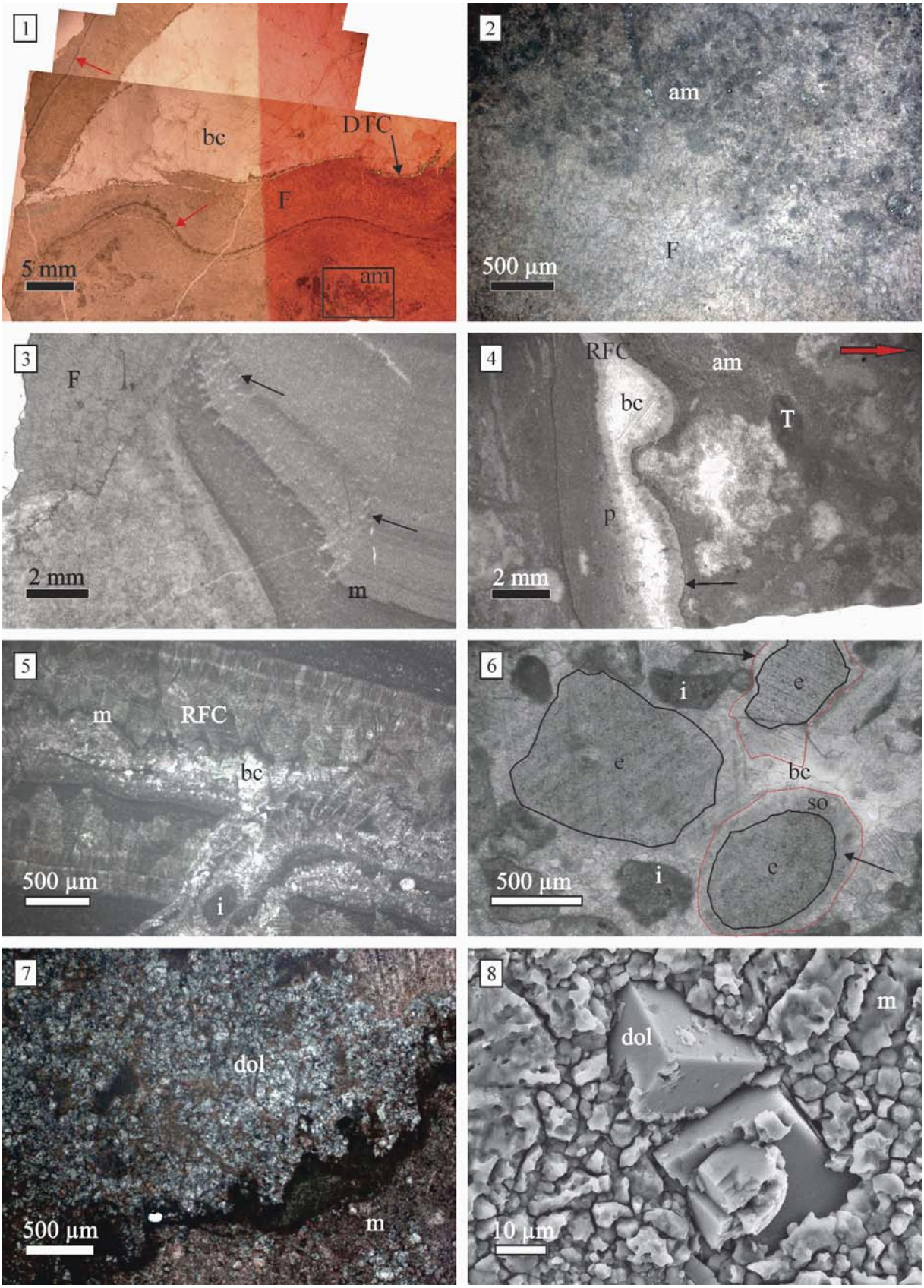

PLATE 8

1 – Diagenetic sequence through a pore: the host is micritic sediment (m), the walls are lined in the upper part by white rhombic crystals of dolomite (dog tooth cement, DTC, remained unstained) and in the lower by fibrous brown cement (F), all cannibalized by large crystals of blocky calcite (bc), lower magnesium after staining (S3, 114D).

2 – The interfingering of the dog tooth cement (DTC) and blocky calcite crystals (bc). SEM photomicrograph (S3, 114D).

3 – The infilling of a pore with drusy cement (bc); non-luminescent micritic matrix (m) and cement crystals showing luminescent overgrowths due to the anoxic fluids from which they precipitated during burial. Cathodoluminescence image (S3, 113A).

4 – Dolomitization front (dol) through a micritic matrix (m) which is crossed by a drusy cement infilling (bc); the dolomite crystals are still not well defined, suggesting an incipient process. SEM photomicrograph (S3, 142B).

5 – Euhedral and subhedral dolomite crystals formed in two stages: non-luminescent nucleus in syndiagenesis and oxygenated environment, and bright-luminescent rims under late diagenesis reducing conditions; a visible transition from dolomitized bands (dol) to muddy matrix (m), poorly dolomitized and nonluminescent. Cathodoluminescence image (S8, 94).

6 – Alternations of bright-fluorescent (macroscopically dark) and non-fluorescent bands through a RFC-filled pore which indicate the organic matter presence which may contributed to the syndepositional cementation. UV fluorescence image (S1, 113B).

7 – Selective dolomitization (dol) affecting only *Tubiphytes* specimes, T (S1, 133).

8 – Intra-granular porosity due by de-dolomitization of dolomite crystals, in first instance affecting the *Tubiphytes* (T) fragment; automicrite (am) patches, fibrous calcite (F) and blocky calcite (bc). Inset, detail showing ghosts of idiomorphic dolomite crystals (S1, 130.13).